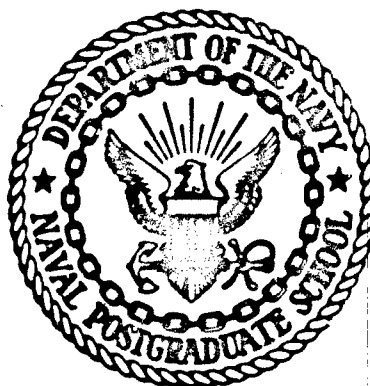2000073/237

NAVAL POSTGRADUATE SCHOOL
Monterey, California

INTERNAL AERODYNAMICS OF TURBOJET TEST CELLS

G. C. Speakman, J. D. Hayes and D. W. Netzer

December 1976

Approved for public release; distribution unlimited

Prepared for:
Naval Air Propulsion Test Center
Trenton, NJ 09628

DDC

FEB 7 1977

RECEIVED

A

NAVAL POSTGRADUATE SCHOOL

Monterey, California

Rear Admiral I. W. Linder   Jack R. Borsting

Superintendent   Provost
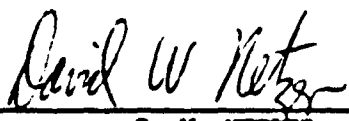

     The work reported herein was supported by the Naval Air Propulsion
Test Center, Trenton, New Jersey, and the Naval Environmental Protection
Data Support Service.

Reproduction of all or part of this report is authorized.

This report was prepared by:

_____   _____
   J. D. HAYES, LT, USN   G. C. SPEAKMAN, LT, USN

              _____
                 D. W. NETZER
              Associate Professor of Aeronautics

Reviewed by: Released by:

_____   _____
R. W. BELL, Chairman   R. R. FOSSUM
Department of Aeronautics   Dean of Research

1

REPORT DOCUMENTATION PAGE	READ INSTRUCTIONS BEFORE COMPLETING FORM

1. REPORT NUMBER NPS-67 Nt 76121	2. GOVT ACCESSION NO.	3. RECIPIENT'S CATALOG NUMBER

| 4. TITLE (and Subtitle)

INTERNAL AERODYNAMICS OF TURBOJET TEST CELLS | 5. TYPE OF REPORT & PERIOD COVERED

Final |
|---|---|
| | 6. PERFORMING ORG. REPORT NUMBER |

| 7. AUTHOR(s)

Glendon C. Speakman
Jack D. Hayes
David W. Netzer	8. CONTRACT OR GRANT NUMBER(s)

| 9. PERFORMING ORGANIZATION NAME AND ADDRESS

Naval Postgraduate School
Monterey, California 93940 | 10. PROGRAM ELEMENT, PROJECT, TASK AREA & WORK UNIT NUMBERS

N623765WR00037 |
|---|---|

| 11. CONTROLLING OFFICE NAME AND ADDRESS

Naval Air Propulsion Test Center
Trenton, New Jersey 09628 | 12. REPORT DATE

December 1976 |
|---|---|
| | 13. NUMBER OF PAGES

63 |

| 14. MONITORING AGENCY NAME & ADDRESS(If different from Controlling Office) | 15. SECURITY CLASS. (of this report)

Unclassified |
|---|---|
| | 15a. DECLASSIFICATION/DOWNGRADING SCHEDULE |

16. DISTRIBUTION STATEMENT (of this Report)

Approved for public release; distribution unlimited

17. DISTRIBUTION STATEMENT (of the abstract entered in Block 20, if different from Report)

18. SUPPLEMENTARY NOTES

19. KEY WORDS (Continue on reverse side if necessary and identify by block number)

Turbojet Test Cell
Augmenter
Flow Model

20. ABSTRACT (Continue on reverse side if necessary and identify by block number)

Elliptic computer codes have been developed (including plot routines) which can be used to study the flow field in test cells and exhaust stacks and in the augmenter tube for low thrust operation. The effects of engine-augmenter spacing, augmenter diameter and inlet design, aft cell wall location, test cell by-pass ratio, cell inlet conditions and stack-augmenter geometry on the flow field and augmenter pressure rise have been calculated. The models appear to be qualitatively correct and adequate for their intended purposes but model validation with experiment is required.

DD FORM 1473 EDITION OF 1 NOV 65 IS OBSOLETE
1 JAN 73
(Page 1)   S/N 0102-014-6601 |

TABLE OF CONTENTS

LIST OF TABLES

LIST OF FIGURES

I. INTRODUCTION

A. Background

Jet engine test cells are employed at all major Naval Air Facilities for maintaining and testing jet aircraft engines. These cells range from older ones which have been converted for use with newer engines at some Air Stations to larger, relatively modern cells at major Rework Facilities. Efficient functioning of these test cells bears directly on the Navy's ability to maintain its aircraft and upon its relation with the surrounding community via noise and air pollution.

A schematic of a typical test cell is shown in Fig. 1. Dimensions of a typical cell are given in Table I.

The function of a test cell is to house the jet engine while it is being run so that adjustments may be made and the engine certified to comply with specifications. The cell must provide a distortion free airflow to the engine inlet and dispose of the engine exhaust gases. Sufficient instrumentation and controls to determine engine performance and to operate the engine are contained in the test cell. The engine may be supported from the floor or walls, or suspended from the ceiling, but in all cases will exhaust into an augmenter tube.

The purpose of the augmenter tube is twofold. First it dilutes the exhaust gas from the engine. This lowers the temperature and kinetic energy of the exhaust gas and preserves the life of the test cell itself. This lower temperature, lower energy gas is then exhausted to the atmosphere. The engine/augmenter acts like a jet pump; the high momentum of the engine exhaust gas entering the augmenter draws secondary air (or augmentation air)

4

along with it. The ratio of augmentation (secondary) mass flow to engine (primary) mass flow is called augmentation ratio. This augmentation ratio is a function of test cell design and of engine placement. The augmentation ratio will be sufficient to cause a pressure rise in the augmenter equal to the pressure drops throughout the balance of the test cell.

The second function of augmentation air is to prevent ingestion of exhaust gases into the engine inlet. A significant ingestion of exhaust gases would seriously degrade the performance of the engine, making any adjustments or evaluation of engine performance meaningless. By having the augmentation air flowing outside the engine from intake to exhaust, it is generally assumed that there will be no recircu_ation of exhaust gases into the engine intake.

Augmentation ratio is critical to the operation of a test cell. Reference 1 points out that if it is too low there is not enough augmentation air to sufficiently cool the exhaust gases or to prevent recirculation and ingestion of the exhaust gases into the engine inlet. If it is too high, excessive cell depression occurs due to the large pressure losses in the flow from intake restrictions (acoustic treatment, flow straighteners, etc.). This cell depression may exceed the structural limits of the test cell. Another problem which results from excessive mass flow through the test cell is engine inlet distortion. Efficient operation of most jet engines requires a pressure distortion at the engine inlet of not greater than two inches of water [Ref. 2]. Excessive flow rates may exceed the capability of the flow straightening devices to reduce all flow irregularities prior to reaching the engine inlet.

5

Current test cell design is more an art than a science. Most analytical work that has been done for predicting the internal aerodynamics of a test cell has been based upon simplified one-dimensional theory. Placement of the engine relative to the augmenter tube is experimentally determined, for example by using ribbons as flow field indicators to show the operator when he is getting secondary flow from engine inlet to exhaust.

Clearly the need for a method of analyzing the internal aerodynamics in a test cell and predicting augmentation ratio, recirculation patterns, and cell velocity distributions is apparent. Utilization of such a method could prevent costly design and construction errors and be used to predict the ability of a given test cell design to handle new engines of different design and flow rate. Also, the effects of cell modification could be investigated without major cost.

B. Pollution Aspects

For non-afterburning engines the temperature of the exhaust gases are sufficiently low so that the chemical reactions are kinetically frozen and the augmentation air merely dilutes the existing pollutants. In this case it is desirable to maximize augmentation air as long as cell pressure is not reduced too far. For example, secondary air injection into the augmenter may be advantageous for dilution without adversely affecting cell pressure. Measurement of pollutant concentrations can be made at the engine exhaust, augmenter exhaust, or the test cell stack exhaust. Flow field visualization (experimental and/or analytical) would be especially helpful for determining where to measure the pollutants and how many samples would be needed to get an accurate measure of the total pollutants emitted. Flow field visualization would also be useful for determining sampling procedures for particulates, which could be centrifuged into a non-uniform distribution due to turning and recirculation in the

6

flow field.

For afterburning engines the exhaust temperatures are high enough to allow chemical reactions to occur outside the engine until the exhaust is water-quenched, typically five to ten feet down the augmenter tube. Since chemical reaction is continuing outside of the engine proper, the amount of augmentation air and the degree to which it mixes and reacts with the exhaust gases will effect the type and amount of pollutants emitted from the test cell. A model which could predict the augmentation ratio, extent of mixing of the two flows and their temperatures could be used to predict pollution levels from test cells and the optimum location for water-quenching, or chemical treatment systems within the augmenter. By utilizing the model to vary the augmentation ratio and point at which the exhaust flow is water-quenched, a test cell design producing a minimum level of pollution could be determined.

C. Analytical Methods

The augmentation ratio can be predicted using one-dimensional theory together with empirical data, such as a jet-spreading relationship for the engine exhaust into the augmenter (Ref. 1). However, these models do not adequately treat the effects of engine-augmenter spacing, nor do they have the ability to indicate whether recirculation is important within the test cell and/or augmenter. In actuality, the flow is three dimensional. However, three-dimensional models to date require excessive computer time and turbulence models are inadequate. For these reasons, two-dimensional models are currently the best compromise for analysis of the flow fields in test cells.

Steady-state flow in a test cell in some cases may be treated similarly to flow in a pipe. Pipe flow is often analyzed assuming a two-dimensional boundary-layer model and solving the parabolic partial differential equations

describing the flow field variables. However, this model requires that there be a single dominant flow direction. This approach may be best suited for the flow within the augmenter since high subsonic velocities can be alternately handled and little if any recirculation regions normally occur. It would not be an effective model for analyzing the flow into a test cell which utilizes a vertical intake or in which strong recirculation zones exist.

General two-dimensional flows, (that is, flows allowing recirculation and flows without a dominant direction), can be described by a set of second-order elliptic partial differential equations. The elliptic models are well suited for the low flow velocities found in engine test cells. However, they are not accurate for the higher velocity engine exhaust and augmenter flows except at low thrust settings.

One approach to the solution of the elliptic equations has been presented by Gosman and Spalding, et. al. [Ref. 3 & 4]. In their method, vorticity (W) and stream function (ψ) are chosen as the dependent variables describing the conservation of mass and momentum. Chosing vorticity and stream function as dependent variables ensures that pressure is eliminated entirely from the equations and that velocity is eliminated as a major factor in the equations. This can provide computational advantages but often causes difficulties when the pressure distribution needs to be accurately determined. Later methods developed by Spalding, et. al. have returned to computations using the primary variables of pressure and velocity.

In the solution of turbulent flows a model is needed which can be used to predict the effective viscosity distribution. Two-parameter models of turbulence (Ref. 5) currently provide reasonable methods for obtaining the effective viscosity distribution within many geometries.

8

The Jones-Launder turbulence model (Refs. 4 and 5) relates the transport properties of the fluid (effective viscosity, μ_{eff}) to two dependent variables, the turbulence kinetic-energy (K) and the turbulence-energy dissipation rate (ϵ) through the relationship

$$\mu_{eff} = C_\mu \rho K^2 / \epsilon$$

where K = turbulence kinetic-energy
ϵ = turbulence-energy dissipation rate
ρ = local density
C_μ = empirically determined coefficient
μ_{eff} = effective viscosity

D. Previous Investigations at NPS

In an earlier study Hayes and Netzer (Ref. 6) used the Spalding, et.al. method for recirculating flows (Ref. 3 and 4) to study the flow field from the engine exhaust to the augmenter exhaust. The elliptic model for axi-symmetric flow was used in order to study the effects of recirculating flows within the test cell which exist near the augmenter inlet. In addition, the model was used for studying the engine exhaust-augmenter flow for low thrust settings. The latter study was needed to determine the effects of augmenter inlet modifications (flanges, etc.) on the augmenter pressure rise.

In some TF-41 test cells a flange has been welded onto the augmenter inlet to restrict the flow area. This lip on the inlet causes recirculation zones in the entrance region of the augmenter. In the study by Hayes and Netzer it was found that at low thrust settings the recirculation zone was of appreciable size and was augmented by the radial inflow of the cell augmention air. At higher augmentation ratios (more secondary air relative to exhaust gas) the recirculation region decreased in size. Thus, at higher thrust settings the recirculation region can probably be neglected and the parabolic models can

9

be properly used for the high exhaust velocities which exist when military thrust and/or an afterburner is employed. It was also found that the length of the inle· lip (i.e., internal diameter of the flange) had only small effects on the shape and size of the recirculation zone within the augmenter and on the augmenter pressure rise at low thrust settings. It may have more effect at the higher thrust settings.

Other variables considered in the study where engine-augmenter spacing and augmenter diameter. The augmenter pressure rise was found to be quite sensitive to augmenter diameter, all other variables being held fixed (i.e. augmentation ratio and diameter of the inlet lip). Increasing the diameter increased the pressure rise within the augmenter. For engine augmenter spacings of 1.5 and 2.5 ft. the augmenter pressure rise did not change appreciably.

From the study it was apparent that the recirculation zones within the test cell (outside of the augmenter) had negligible effects on the augmenter pressure rise. However, these recirculation zones are important in determining whether exhaust gas can be ingested into the engine inlet. In general, it was found for idle conditions with an augmentation ratio of 0.5 that the engine exhaust jet spread to its maximum diameter at approximately two augmenter diameters from the augmenter inlet. The engine exhaust gases and the augmentation air were well mixed between 3.5 and 4 augmenter diameters from the augmenter inlet. This was also the location to reach the maximum pressure within the augmenter. The minimum pressure occured at approximately one-third of a diameter from the augmenter inlet.

For idle conditions and a 1.5 ft engine-augmenter separation, the augmenter pressure rise decreased linearly from 47 psf to 36 psf as the augmentation ratio was increased from 0.5 to 1.0.

Several additional studies were required with the model. The effect of moving the engine exit flush with the augmenter inlet was not determined. Also, the effects of moving the aft test cell wall forward to the augmenter inlet plane was not determined. A limitation of the initial model was that the velocity profile within the test cell was specified at the engine-exhaust plane. A more realistic boundary condition would be to specify a uniform velocity profile in the test cell at the plane of the engine inlet.

One major limitation of the model, which results from using the transformed variables of vorticity and stream-function, is the sensitivity of the predicted pressure distribution to the stream-function (ψ) distribution. Very small changes in ψ can cause large errors in the predicted pressure field. This limitation, plus the limitation of employing the elliptic equations only for low subsonic Mach numbers, points to the necessity for using the parabolic methods and primary variables for the engine-augmenter flows at high trust settings. However, the model does provide a valuable tool for low thrust settings and for the recirculating flows within the test cell. In addition, the model was needed to determine whether or not the recirculation zone within the augmenter inlet could be neglected, i.e. whether or not the parabolic model would be applicable.

Because the equations for subsonic, recirculating flows are elliptic in nature, boundary conditions must be specified around the entire flow field. This prohibits augmentation ratio from being a dependent variable directly in the analysis. The analysis is independent of the inlet/exhaust designs of a particular test cell. However, the output data from the model can be used in conjunction with the conservation equations for the entire test cell to determine the augmentation ratio. The inlet/exhaust treatment devices used in a particular test cell will determine the closure for the complete analysis.

11

The model does have the ability to calculate the internal aerodynamics under these restrictions. The accuracy of the model needs to be determined by direct comparison with test cell data.

E. Present Investigation

As discussed above, several additional studies were required with the elliptic model. The present study used the model to investigate the effects of (a) moving the specified cell inlet velocity profile from the engine exhaust plane to the engine inlet plane, (b) moving the augmenter forward to be flush with the engine exhaust plane, and (c) moving the art wall of the test cell forward to be flush with the augmenter inlet plane.

An axi-symmetric representation of the cell inlet and test section models the cell and engine/augmenter as three concentric pipes of differing size (Fig. 2a). The advantage to this representation is that the size of the pipes correspond exactly to the size of the actual components that they represent. This allows a realistic solution of the flow field in the area of the engine inlet and exhaust and the augmenter inlet. While the test cell has a rectangular shape, modeling this as a circular pipe should not introduce any significant errors if the engine is not located too near the test cell floor.

The flow in test cells is generally not symmetric about its center-line. The flow into the test cell usually enters from above and at right angles to the test portion of the cell. Additionally, the augmenter, and therefore the engine, are not located symmetrically in the cell. Their location is typically much nearer the floor of the test cell than the ceiling.[1] This lack of

_____

[1] NARF Alameda and NARF North Island test cells have the engine/augmenter center line five feet from the floor and thirteen feet from the ceiling.

symmetry causes the axi-symmetric representation to be unrealistic in the areas of the test cell inlet and exhaust stack and ignores any effects of non-symmetrical augmenter location. Flow field visualization in these areas is of interest for examining test cell inlet distortion and exhaust stack velocity profiles. A meaningful gas sampling requires knowledge of the velocity profiles unless a large number of samples can be taken across the flow field.

A two-dimensional planar representation of the test cell models it as a series of planes, one inside the other (Fig. 2b). Thus, the engine inlet and exhaust and the augmenter inlet can be thought of as slots, extending the entire width of the test cell.

If the height of the "2-D engine" is taken as the diameter of the actual engine, and if velocity is unchanged, then the mass flow rate through the engine is not correct. Conversely, if the mass flow rate and velocity are to be unchanged in the 2-D model, then the engine and augmenter are represented as extremely thin rectangular shapes in the planar model. This size distortion of the engine and augmenter may cause the flow field in the immediate area of the engine inlet and exhaust and augmenter inlet to be unrealistic. This scaling will also cause some difficulties with modeling diffusion rates since flow gradients are also distorted. Neither of the two methods is entirely satisfactory near the engine since in this region in the actual conditions the flow transitions from planar to nearly axi-symmetric. However, the planar model is suitable for the test cell inlet and exhaust stack and should yield at least qualitative behavior in the regions near the engine.

Due to the two-dimensional limitation, both the planar and axi-symmetric representations suffer from their inability to allow interaction of the flow above the engine with the blow beneath the engine. The axi-symmetric

13

formulation suffers from the assumption that the flow is symmetric the entire length of the model and the planar representation is limited in that once the proportion of air flowing beneath the engine is specified, it cannot change.

Since the main area of interest in the present study was the flow field for the entire test cell, and not primarily the interaction of the engine exhaust and augmenter inlet, the planar representation was chosen for both the inlet/test section and the exhaust stack section of the test cell. It was also decided to keep the mass flow rates and velocities in the model equal to those in the actual test cell. As discussed above, this necessitated the use of an "engine" and "augmenter" with reduced height in the 2-D model.

II METHOD OF INVESTIGATION

A. Axi-symmetric Model

The first modification to the model (Ref. 6) was to move the specified "inlet" to the test cell. In the original model this "inlet" was located at the engine exhaust plane and the cell flow velocity was assumed to increase linearly from the ceiling to the engine wall. The "inlet" was moved to the engine inlet plane where a uniform inlet velocity could be realistically assumed. The results of this modification were compared to the earlier results.

The modified model was then used to determine the effects of zero spacing between the engine and augmenter on the augmenter pressure rise. In addition, the effects of moving the aft cell wall to the plane of the augmenter inlet were investigated.

B. 2-D Planar Model

The equations, appropriate boundary conditions, and solution procedures are essentially identical to those presented in reference 6. Some changes were required in initial conditions and relaxation parameters in order to insure convergence. The 2-D planar geometries employed for the test cell and exhaust stack are presented in Figures 3 and 4 respectively. The model was used to study the effects of engine flow rate, augmentation ratio and augmenter position in the exhaust stack on the flow fields within the test cell and exhaust stack.

15

III RESULTS AND DISCUSSION - AXI-SYMMETRIC MODEL

Moving the "inlet" for the model from the engine exhaust plane to the
engine inlet plane and changing the specified velocity profile from linearly
increasing to uniform had no appreciable effect on the flow field and pressure
rise within the augmenter. Thus, repetition of the earlier test conditions
(Ref. 6) was not necessary.

Moving the augmenter flush with the engine exit also did not change the
augmenter pressure rise from that found with a 1.5 ft. separation. Larger
spacings (Ref. 6) were found to decrease the pressure rise. These results
indicate that for idle conditions, the augmenter pressure rise is only slightly
sensitive to engine-augmenter spacing. For military thrust and/or afterburner
conditions (to be studied using the parabolic model) it would be expected
that engine-augmenter spacing would have a much larger affect on augmenter
pressure rise.

Test cell design may affect augmenter pressure rise and exhaust gas
recirculation. However, moving the aft test cell wall forward to the augmenter
inlet plane did not change the augmenter pressure rise (for idle conditions and a
0.5 augmentation ratio) and changed the recirculation regions only slightly
near the augmenter inlet.

The primary value of the axi-symmetric model is that it can be used to
realistically study the affects of augmenter inlet design and test cell geometry
on the recirculation within the test cell and on the augmenter pressure rise.
The major weaknesses of the model are (a) it is limited to low subsonic engine

16

exhaust velocities, (b) pressure rise calculations are very sensitive to the stream-function solution, and (c) non axi-symmetric flows (cell-stack intersection, engine location within the test cell, etc.) cannot be adequately investigated.

The restriction to low subsonic velocities results from the use of elliptic equations. Since the recirculation zones (both within the test cell and augmenter) were found to have only a small affect on augmenter pressure rise, parabolic equations can be utilized to investigate the affect of high subsonic to sonic engine exit velocities on augmenter pressure rise and mixing. This work is currently being conducted. The solution to the second problem can be obtained by returning to the primary variables of velocity and pressure rather than using the transformed variables of vorticity and stream function. Future investigations will be directed toward this approach. The third problem cannot be handled with an axi-symmetric model. It was for this reason that the 2-D planar study was made.

IV. THE 2-D PLANAR MODEL

A. Cell Geometry

The solution procedure utilizes a variable grid size. It was desirable
to space the grid closely together in areas where the flow field was expected
to be changing significantly and gradients would be high. These areas are
near boundaries and around the engine exit and augmenter inlet. In other
regions the grid size was allowed to expand, reducing the total number or
grid points and thus conserving computer time without sacrificing accuracy.

The entire test cell was determined to be too large and unwieldy to
model in one program. Thus, it was divided into two areas of interest, the inlet
and test portion of the cell and the exhaust portion of the cell.

The inlet and test portion of the cell, hearafter referred to as the
cell test area, was taken as the rectangular area from and including the test
cell inlet to the far wall enclosing the augmenter tube (Fig. 3). This allowed
study of the flow into the test cell, as it made a right-angle turn, as well as
the flow around the engine and augmenter. In this study the flow field was
not calculated in the augmenter itself.

The exhaust stack of the test cell was considered to be the rectangular
area of the actual exhaust stack (Fig. 4). The flow was not calculated in the
augmenter tube. The velocity profile was assumed uniform at the augmenter tube
exit. This study ignored the presence of any acoustic baffles or air pollution
devices in the exhaust stack.

18

B. Parametric Study

The computer models were used to study the large test cells at the Naval Air Rework Facility, Alameda (Table I). The flow rates and basic augmentation ratio used were for the Allison TF-41 turbo-fan engine. The engine flow rates and temperatures are given in Table II. A summary of runs made and parameters varied is given in Table III.

1. Model Parameters

The sensitivity of the model to various assumptions was investigated first. Three initial runs (J1, J3, J4) were made to which all additional runs could be compared.

(a) Augmenter Inlet Velocity Profile

The effect of different velocity profiles in the augmenter intake was investigated by fixing the velocity profile rather than letting the program calculate it. The first profile (runs G1, G4) investigated was that obtained experimentally in a study by Bailey (Ref. 1). The second profile (runs H8, H9) assumed was plug flow.

(b) Stream Function On Engine Walls

In a 2-D planar model, the amount of flow under and over the engine must be specified. Since this was an arbitrary selection, four runs (I1, I2, I3, I4) were made varying the percent of augmentation air mass flow below the engine from 16% to 36%. Twenty-six percent corresponded to uniform flow.

(c) Inlet Turbulence Level

Turbulence kinetic-energy at the cell inlet and the engine exhaust was increased by a factor of 25. These runs (L1, L2) were conducted at both idle and military thrust.

19

(d) Cell Test Area Augmentation Ratio

The effects of augmentation ratio on cell flow patterns and recircu-
lation were investigated. Runs were made at augmentation ratios of 0.25
(K1, K4), 0.5 (K2, K5) and 1.0 (J1, J4) at idle thrust and at military thrust.
A single run (K3) at idle thrust and an augmentation ratio of 1.5 was also made.

(e) Geometry

In the cell exhaust area, three runs (A2, A3, A4) were made with the
augmenter tube flush with the exhaust stack wall at different power settings.
The augmenter tube was then extended four feet into the exhaust stack and
three additional runs (C2, C3, C4) were made at the equivalent power settings.

Geometry was not varied for the cell test area.

V. RESULTS AND DISCUSSION - 2-D PLANAR MODEL

A. General Discussion

For each run the distribution of stream function was punched on IBM cards. They were then run through a subroutine which converted the results from the non-uniform grid of the program to a uniform grid suitable for plotting by the NPS Computer Library Routine, CONTUR. The graphs are distorted by a doubling of the height in order to display the flow field more clearly.

In each graph of stream function distribution ten streamlines (lines of constant stream function) evenly spaced across the cell inlet were plotted. Using the same spacing an additional two streamlines below the lowest value at the cell inlet and four streamlines above the highest value of the cell inlet were plotted. These allowed display of zones of recirculation. Plotting the same number of streamlines uniformly spaced in each case facilitated comparison among the plots. In the cell test area an additional two streamlines, those which were specified on the upper and lower engine walls, were plotted.

The flow field displayed in Figures 5 through 22 are for the cell test area. The flow enters the test cell from above and smoothly turns to parallel the cell floor and ceiling. An area of recirculation forms in the lower left-hand corner. Midway between the cell inlet and engine inlet the flow is uniform across the cell. The engine then draws flow into its inlet and the augmentation flow is drawn into the augmenter. This causes small areas of recirculation on the cell walls above and below the engine intake.

As the flow nears the augmenter intake it "necks down" further until it is entrained with the engine exhaust in the augmenter. Due to viscous forces on the neighboring air, an area of recirculation is formed above and below the augmenter intake. Above the augmenter inlet there is normally just one large recirculation zone. Below the inlet there are three zones. The first is fairly strong and directly below the intake. The second and third are weak, and continue back to the right-hand wall.

In all instances the streamlines behaved in a reasonable manner and in general agreed with what was expected. The effect of the cell inlet flow and the effect of placing the engine/augmenter nearer one wall than another could be seen in the recirculation patterns.

In the case of the exhaust stack the streamlines show (Figures 23-28) two large recirculation zones on either side of the high velocity inlet stream. The flow turns to become parallel to the stack walls. The flow across the stack exit plane is non-uniform and in all cases the exit velocity is approximately 80% higher near the outer ("lower" in the figures) wall than the inner.

Diffusion causes exhaust gases to enter the recirculation zones above and below the augmenter inlet. Convection in the recirculation zones carries the exhaust gases to the forward portion of the recirculation region. From this point the exhaust gases may again diffuse forward in the cell.

Calculations were made for the distribution of engine exhaust gas within the test cell. Although the qualitative behavior of the mass-fraction distribution was reasonable, the quantitative values were not. The source of this error appears to lie in the choice of the planar geometry to model the test cell.

Since it was decided to size components to maintain the proper mass flow ratios and velocities of a test cell, the dimensions of the engine/augmenter had to be severely reduced in the planar representation. This, together with the use of only three grid points in the engine exit plane, resulted in the gradients of the variables being extremely and unnaturally high in the region of the engine exhaust/augmenter inlet. These high gradients caused unrealistically high diffusive transport in the program. For these reasons, the mass fraction distributions are not presented.

B. Specific Parametric Results

1. Engine Power Settings

Comparing Figs. 5, 6, and 7, little change is noted until 100% RPM is reached. At 100% the recirculation region has moved forward and would cause increased exhaust gas ingestion (for fixed augmentation ratio). In actual operation augmentation ratio would increase with RPM if the engine-augmenter spacing remained constant. Since the results for 90% and idle RPM were nearly identical, only 100% and idle RPM were examined in subsequent comparisons.

2. Augmenter Inlet Velocity Profile

Figures 5 and 7 (augmenter velocity profile calculated), 8 and 9 (experimental augmenter velocity profile) and 10 and 11 (plug flow) show the effect of the assumed augmenter inlet velocity profile on numerical results. At idle thrust all three cases produced similar flow distribution. At military thrust the two fixed profile cases remained similar, not only to each other but also to their idle thrust distributions. However, the calculated velocity profile case showed a larger and stronger upper recirculation zone.

Cell inlet flow fields were nearly identical for the three cases at each power setting.

23

3. Stream Function on Engine Walls

   (a) Idle Thrust (Figs. 5, 12 and 14)

   The recirculation zones above and below the engine were the main differences in these runs. With increasing specified flow above the engine the recirculation zone there got smaller and less intense. However, reducing recirculation on one side of the engine/augmenter merely increased it on the other.

   (b) Military Thrust (Figs. 7, 13 and 15)

   In the case of military thrust both increasing and decreasing the mass flow beneath the engine resulted in an increase in size and intensity of the recirculation zones both above and below the engine.

4. Inlet Turbulence

   (a) Idle Thrust

   Increasing the turbulent kinetic-energy at the cell inlet and the engine exhaust had little effect on the cell inlet area (see Figs. 5 and 16) but decreased the size and intensity of the recirculation zones around the engine/augmenter somewhat.

   (b) Military Thrust

   In this case (Figs. 17 and 22) increasing turbulent kinetic-energy caused the size of the recirculation zone in the cell inlet to be reduced considerably. The size and intensity of the recirculation zones above and below the engine/augmenter were also reduced, a ias the case at idle thrust.

   These results indicate that flow conditioning within the cell inlet stack and the turbulence level in the engine exhaust can affect exhaust gas entrainment into the engine inlet.

24

5. Augmentation Ratio

(a) Idle Thrust

For augmentation ratios of 1.0 and 1.5 at idle thrust (Figs. 5 and 20) there was little difference in the flow field. The intensity and forward limits of the recirculation zones were similar, although their shapes were different.

When augmentation ratio was reduced to .5 (Fig. 19), the recirculation zone increased considerably in intensity and moved forward significantly, especially above the engine. This would increase the level of exhaust gas ingestion into the engine intake.

Further reduction in augmentation ratio to .25 (Fig. 18) resulted in the recirculation zone moving further forward to such an extent that a second upper recirculation zone was formed.

(b) Military Thrust

As the augmentation ratio was lowered from 1.0 to .5 at military thrust (Fig. 7, and 22) the intensity of the recirculation zones increased and they moved slightly forward. With an augmentation ratio of .25 (Fig. 21), there was a further forward movement of the recirculation zones.

Qualitatively the model indicated there is a possibility of excessive exhaust gas ingestion at low augmentation ratios with existing cell designs.

6. Geometry of Augmenter in Exhaust Stack (Figs. 23-28)

There was little difference among the plots. The high inlet velocity tended to maintain itself until at least halfway across the stack. Thus, the presence of the augmenter tube extending into the cell had little effect on the overall pattern in the exhaust stack. This was true for all power settings from idle thrust to military thrust.

25

VI. CONCLUSIONS

A. General

Two elliptic models have been developed for flow field analysis of turbojet test cells. The models provide valuable tools to aid in test cell design and modification as often required for adaptation to new engines and for pollution control. The models can be used for prediction of the effects of many engine test conditions and cell geometries on the velocity and pressure fields and the exhaust gas distribution. Within the augmenter tube the models are limited to low subsonic flows because of the elliptic nature of the equations. The models yield results which are in qualitative agreement with experiment. Quantitative model verification is required. The models are two-dimensional, as as such, cannot be used to evaluate three dimensional phenomena such as the interaction of flow below the engine with that above the engine.

B. Axi-symmetric Model

The axi-symmetric model has been employed to examine the effects (at low engine thrust) of engine-augmenter spacing, augmenter diameter and inlet construction, aft cell wall location, and test cell by-pass ratio on the velocity, temperature, mass fraction and pressure distributions within the test cell and augmenter tube.

Augmenter inlet modifications (such as flanges, etc.) were found to affect the flow field within the augmenter for low thrust, low augmentation conditions. At higher augmentation ratios the effects are significantly reduced. Augmenter pressure rise was sensitive to augmenter diameter but was rather insensitive to engine-augmenter spacing for low thrust conditions.

26

Aft test cell wall location affects the recirculating flow regions in the test cell which may affect exhaust gas ingestion at low cell augmentation ratios. However, the aft wall location did not significantly affect the augmenter pressure rise.

At low thrust settings the engine exhaust and augmentation air were well-mixed at 3.5-4 augmenter diameters within the tube and the augmenter pressure rise peaked at this location. The minimum pressure occurred at approximately 0.3 augmenter diameters within the tube. Augmenter tube modifications may be possible which utilize secondary air ingestion to quench or dilute the exhaust gases with minimum effect on the cell augmentation ratio.

The predicted augmenter pressure rise was insensitive to the specified test cell inlet velocity profile and to the location of the "inlet" to the cell.

C. 2-D Planar Model

The 2-D planar model has been used to examine the effects of engine location, cell inlet conditions, and exhaust stack-augmenter geometry on the flow field.

For the cell flow velocities investigated (four ft./sec. to 16 ft./sec.) there is apparently little need for turning vanes or flow straightening devices in the cell test area itself in order to achieve a uniform flow field prior to the engine intake. However, cell inlet turbulence was found to considerably affect the size and intensity of recirculating flows within the test cell. The model also indicated that there is the possibility of appreciable exhaust gas ingestion at the low thrust, low cell augmentation ratio conditions in existing test cells.

27

The cell exhaust stack velocity was found to be very non-uniform, suggesting that care must be used in sampling for particulates in the exhaust stack exit plane. The distance that the augmenter tube extended into the exhaust stack had little affect on the exhaust plane velocity field.

D. Future Work

The models appear to be adequate for their intended purposes but model verification is required. In addition, the augmenter tube flow field and pressure rise calculations need to be performed for the high thrust/afterburning conditions. For these reasons current work is being done in both experimental and analytical areas.

A one-eighth scale test cell is being constructed which can be utilized to validate/improve models and to perform basic studies to determine the effects of test cell/augmenter design and engine operating conditions on the quantity and distribution of exhaust stack pollution. The test cell will also provide an inexpensive means for evaluating new pollution control and measurement methods.

A parabolic model is also being developed which can be used to analyze the augmenter flow field for the high thrust, high cell augmentation ratio conditions.

VII. REFERENCES

1. Bailey, D. L., Tower, P. W., and Fuhs, A. E., AGARD Preprint No. 125, Atmospheric Pollution by Aircraft Engines, "Pollution Control of Airport Engine Test Facilities".

2. Flight Propulsion Division of General Electric, "Airline Planning Guide: Test Facilities for Large Advanced Turbojet and Turbofan Engines", 1 April 1967.

3. Gosman, A. D., Pun, W. M., Runchal, A. K., Spalding, D. B. and Wolfshtein, M., Heat and Mass Transfer in Recirculating Flows, Academic Press, 1969.

4. Spalding, D. B., Gosman, A. D., and Pun, W. M., "The Prediction of Two-Dimension Flows", Short Course, Pennsylvania State University, August 1972.

5. Launder, B. E. and Spalding, D. B., Lectures in Mathematical Models of Turbulence, Academic Press, 1972.

6. Hayes, J. D. and Netzer, D. W., "An Investigation of the Flow in Turbojet Test Cells and Augmentors", Naval Postgraduate School Report, NPS-57Nt-75101, Oct. 1975.

TABLE I

JET ENGINE TEST CELL DIMENSIONS

Cell Test Area:

length	82.0'
depth	24.0'
height	18.0'

Inlet Stack:

height above cell ceiling	34.0'
depth	24.0'
width	12.0'

Engine/Augmentor Centerline:

distance from floor	5.0'
distance from walls	12.0'

Augmentor:

length (for TF-41 engine test)	13.25'
inlet diameter	3.5 '
overall diameter	6.0 '

Engine (TF-41):

length (including bellmouth)	17.25'
bellmouth diameter	3.75'
engine diameter	3.1 '
exhaust plane diameter	2.1 '

Distance from engine exhaust plane to augmentor inlet plane	1.5 '

Cell Exhaust Area:

height	54.0 '
depth	18.0 '
width	12.0 '

Augmentor Centerline:

distance from floor	8.0 '
distance from walls	9.0 '

Augmentor:

distance into exhaust stack	4.0 '
diameter	6.0 '

30

TABLE II

ENGINE OPERATING CONDITIONS

RPM Setting	Turbine Outlet Temperature °R	Exhaust Plane Temperature °R	Mass Flow lbm/sec
100%	1524	1001	263
90%	1362	924	200
Idle *	1100	800	100

* Approximate

TABLE III

COMPUTER RUNS: ENGINE AND TEST CELL CONDITIONS

RUN NO.	FIG. NO.	POWER SETTING	AUGMENTATION RATIO	AUGMENTER VELOCITY PROFILE	PERCENTAGE AUGMENTATION AIR BELOW ENGINE	REMARKS
J1	5	IDLE	1.0:1	CALCULATED	26	
J3	6	90%	1.0:1	CALCULATED	26	
J4	7	100%	1.0:1	CALCULATED	26	
G4	8	IDLE	1.0:1	EXPERIMENTAL	26	
G1	9	100%	1.0:1	EXPERIMENTAL	26	
H8	10	IDLE	1.0:1	PLUG FLOW	26	
H9	11	100%	1.0:1	PLUG FLOW	26	
I1	12	IDLE	1.0:1	CALCULATED	16	
I2	13	100%	1.0:1	CALCULATED	16	
I3	14	IDLE	1.0:1	CALCULATED	36	
I4	15	100%	1.0:1	CALCULATED	36	
L1	16	IDLE	1.0:1	CALCULATED	26	INLET BOUNDARY TURBULENCE KINETIC ENERGY = 25 TIMES NORMAL
L2	17	100%	.5:1	CALCULATED	26	

TABLE III (Continued)

RUN NO.	FIG. NO.	POWER SETTING	AUGMENTATION RATIO	AUGMENTER VELOCITY PROFILE	PERCENTAGE AUGMENTATION AIR BELOW ENGINE	REMARKS
K1	18	IDLE	.25:1	CALCULATED	26	
K2	19	IDLE	.5:1	CALCULATED	26	
K3	20	IDLE	1.5:1	CALCULATED	26	
K4	21	100%	.25:1	CALCULATED	26	
K5	22	100%	.5:1	CALCULATED	26	
A2	23	IDLE	.5:1	-------	--	AUGMENTER FLUSH WITH EXHAUST STACK WALL
A3	24	90%	.5:1	-------	--	
A4	25	100%	.5:1	-------	--	
C2	26	IDLE	.5:1	-------	--	AUGMENTER EXTENDS 4 FT INTO EXHAUST STACK
C3	27	90%	.5:1	-------	--	
C4	28	100%	.5:1	-------	--	
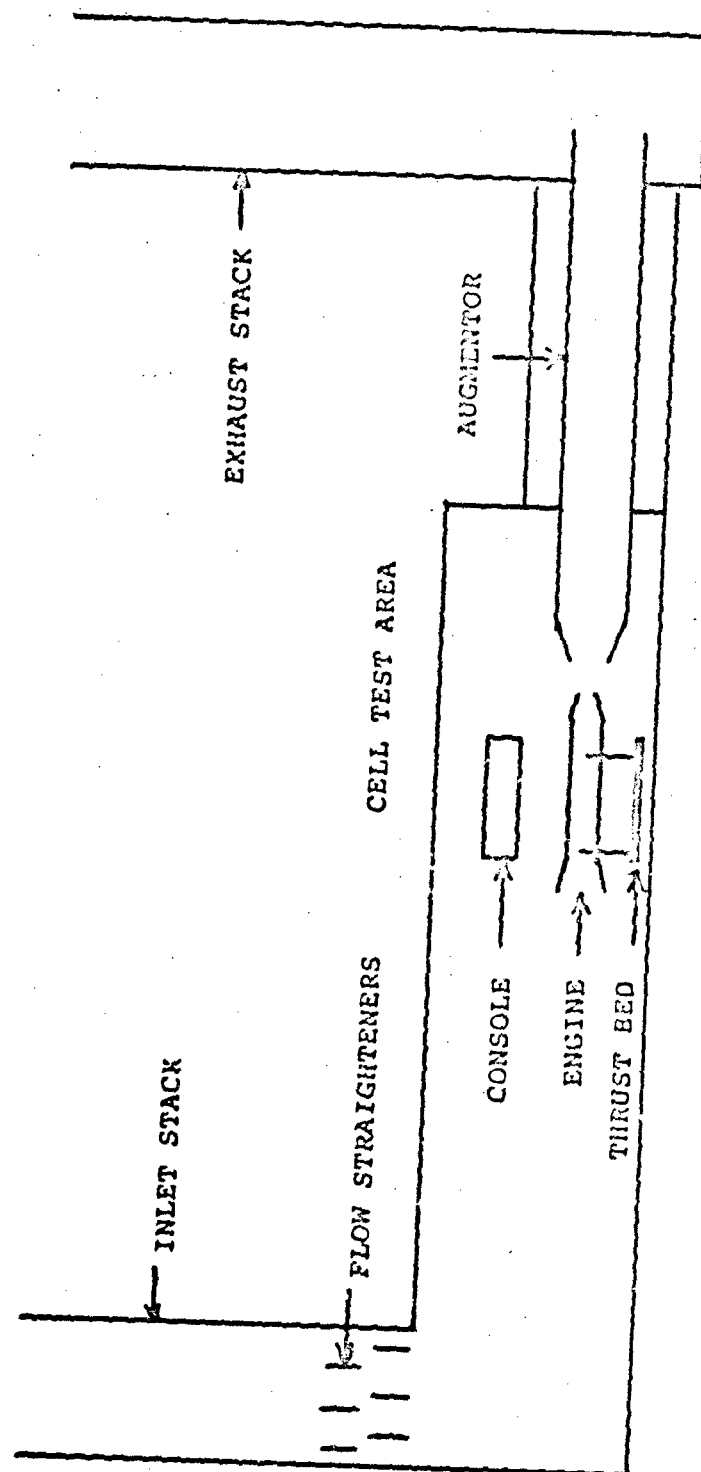
FIGURE 1. TYPICAL TURBOJET TEST CELL.

34
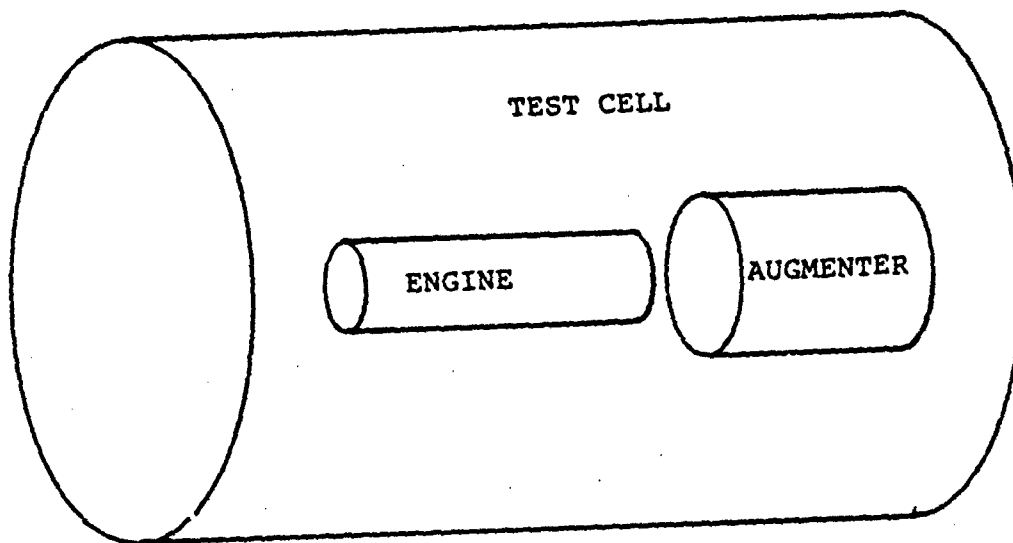
FIGURE 2a. AXI-SYMMETRIC REPRESENTATION OF ENGINE/AUGMENTER
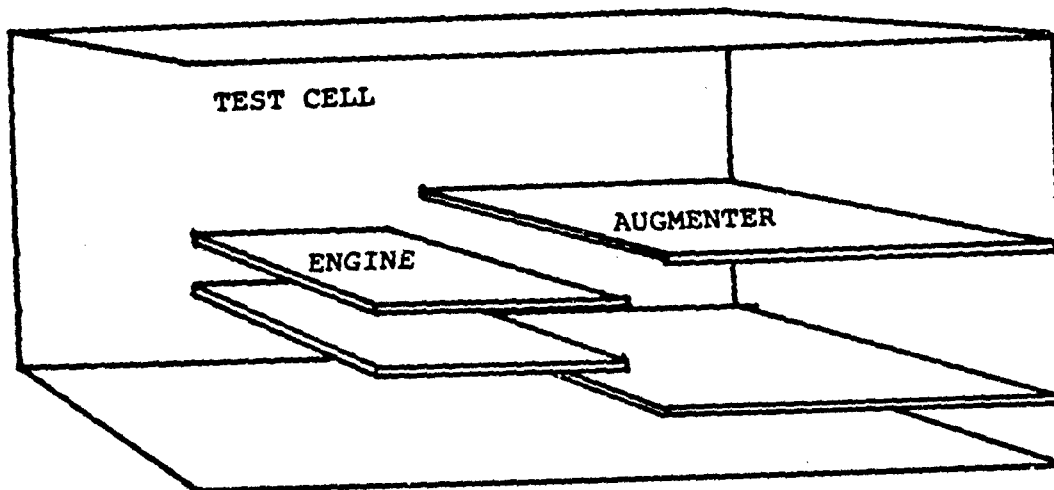
FIGURE 2b. PLANAR REPRESENTATION OF ENGINE/ AUGMENTER
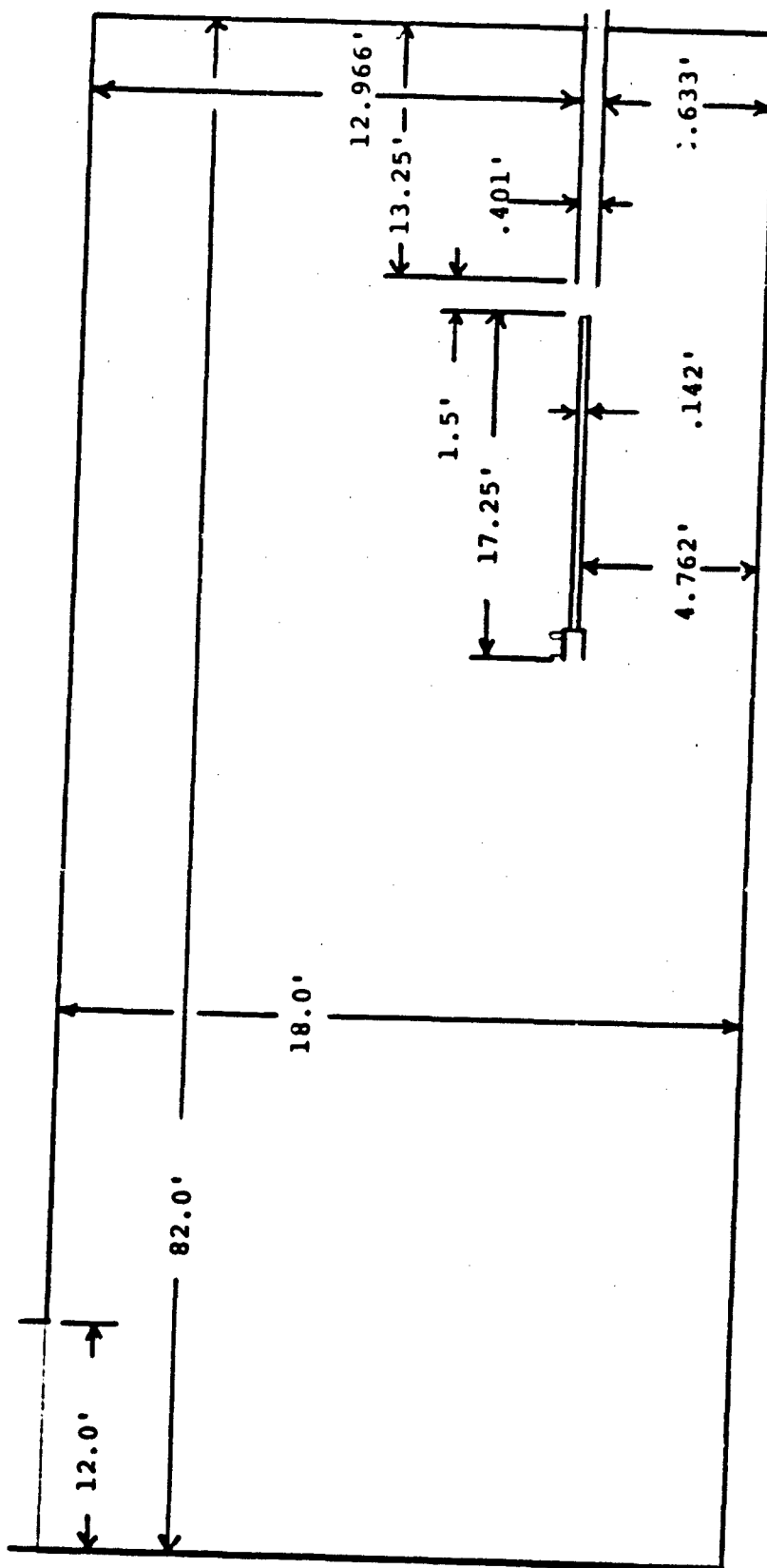
FIGURE 3. GRID OUTLINE OF CELL TEST AREA WITH DIMENSIONS; ENGINE, AUGMENTER AND CELL WALLS ARE SHOWN.
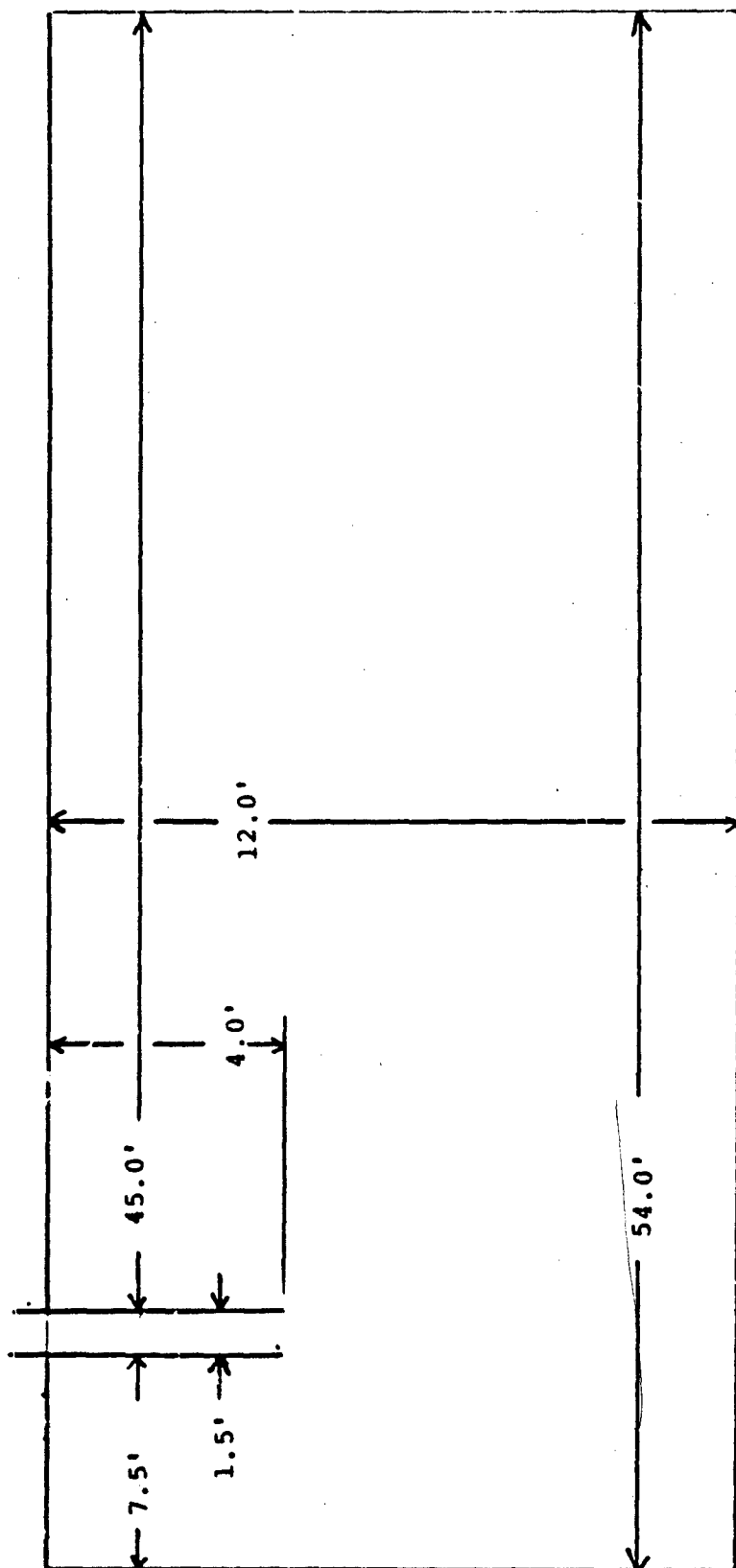
FIGURE 4. GRID OUTLINE OF CELL EXHAUST AREA WITH PROGRAM DIMENSIONS:
AUGMENTER AND CELL WALLS ARE SHOWN.
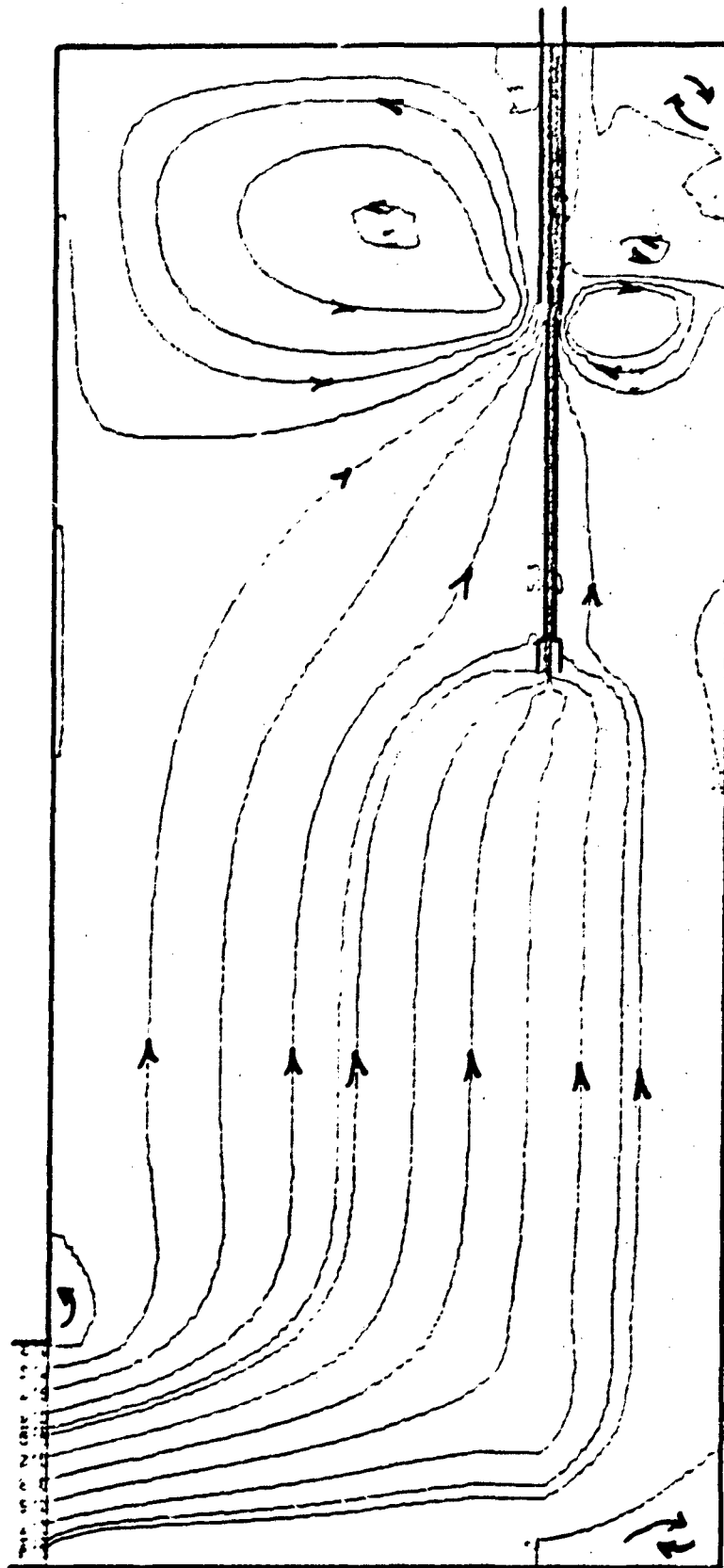
FIGURE 5.   DISTRIBUTION OF STREAMLINES   RUN J1:   Idle RPM,
AUGMENTATION RATIO = 1.0:1.
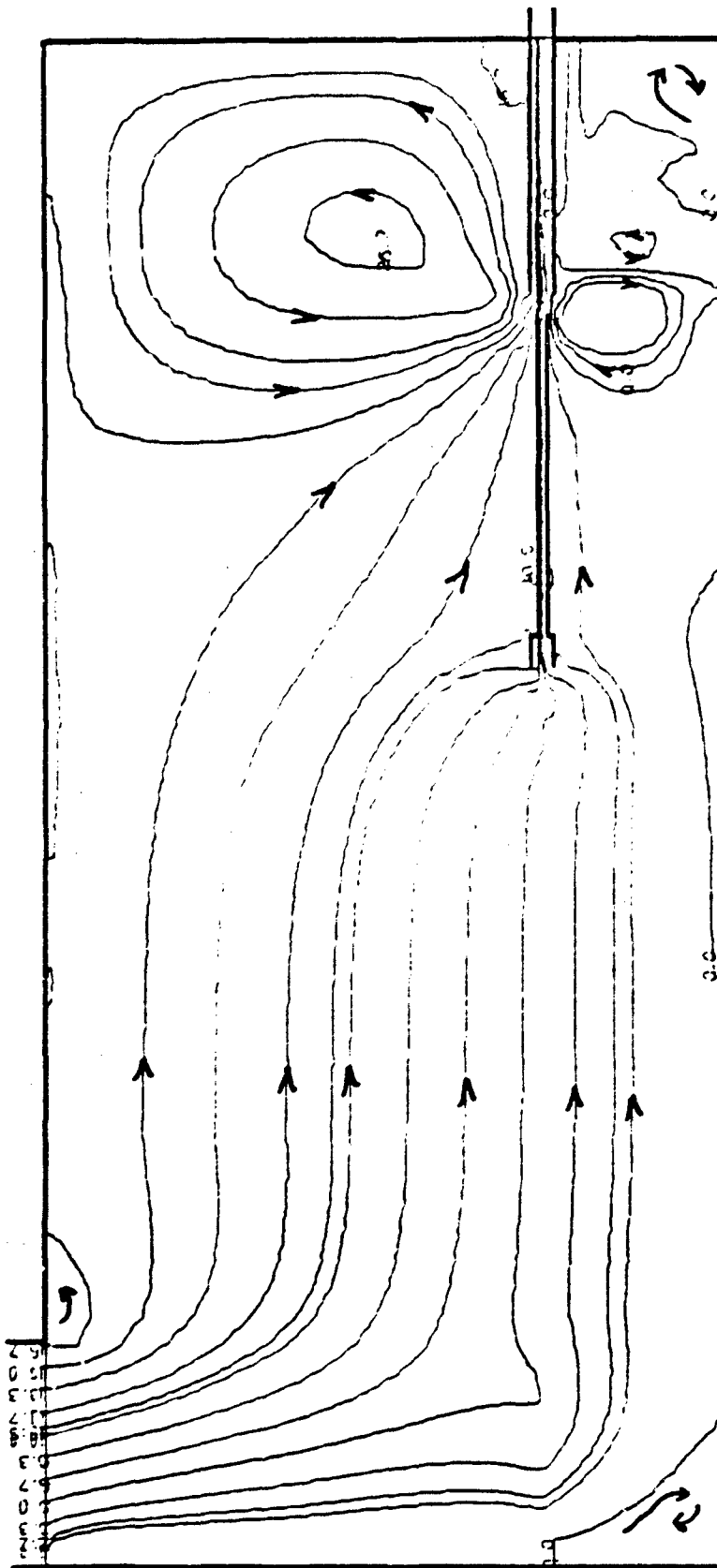
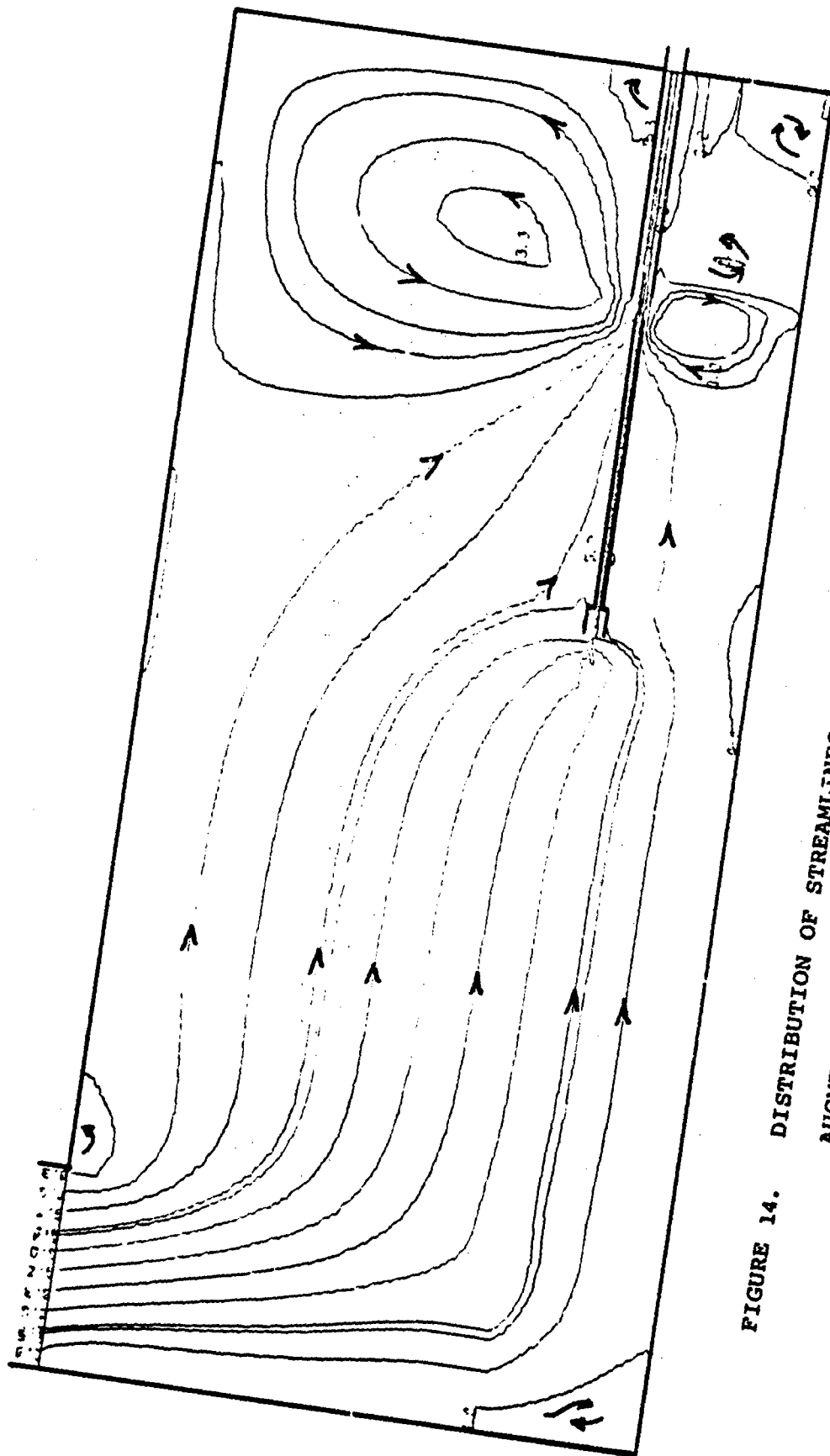FIGURE 6. DISTRIBUTION OF STREAMLINES RUN J3: 90% RPM, AUGMENTATION RATIO = 1.0:1.
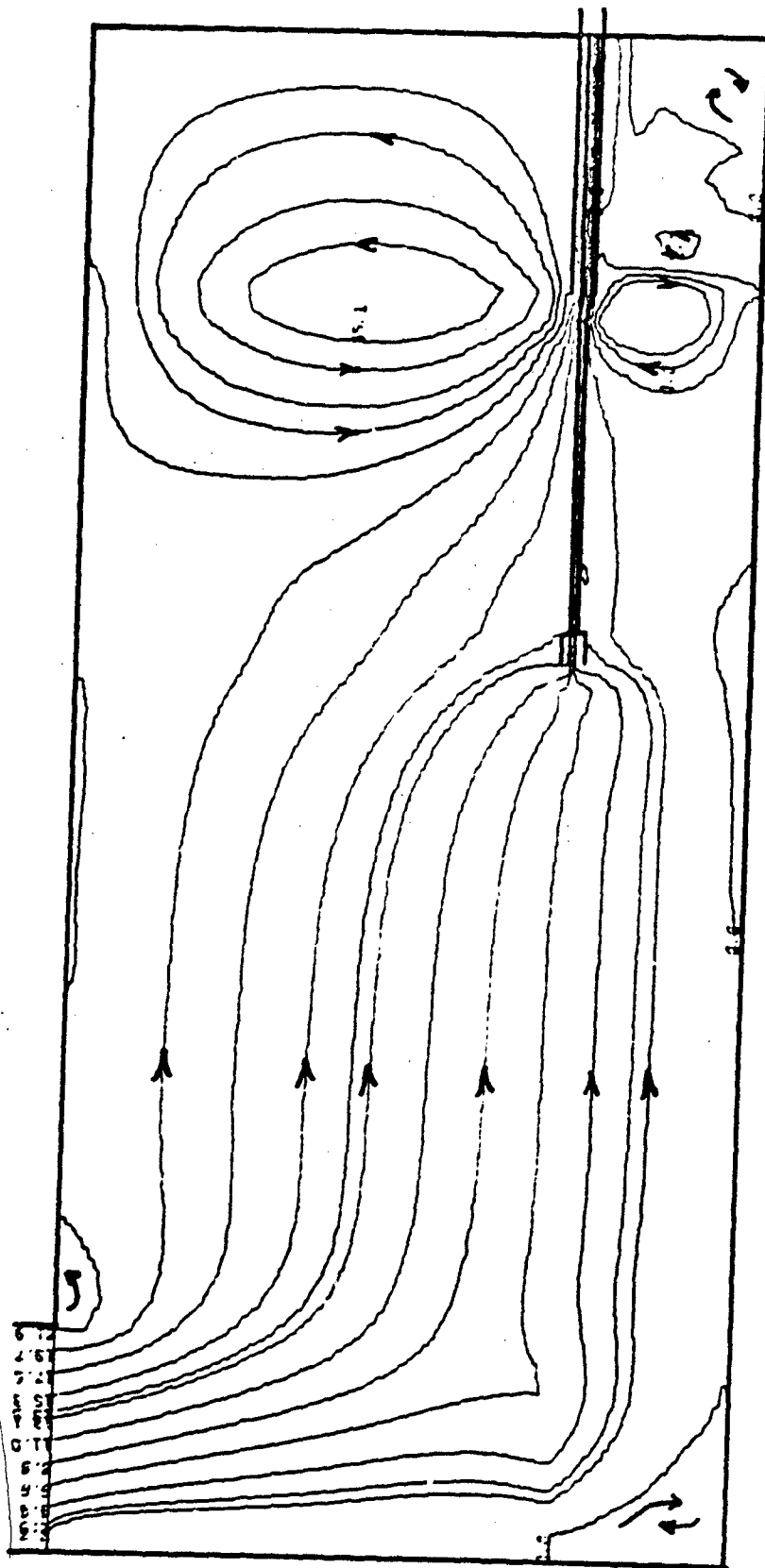
FIGURE 7.   DISTRIBUTION OF STREAMLINES   RUN J4:   100% RPM,

AUGMENTATION RATIO = 1.0:1,
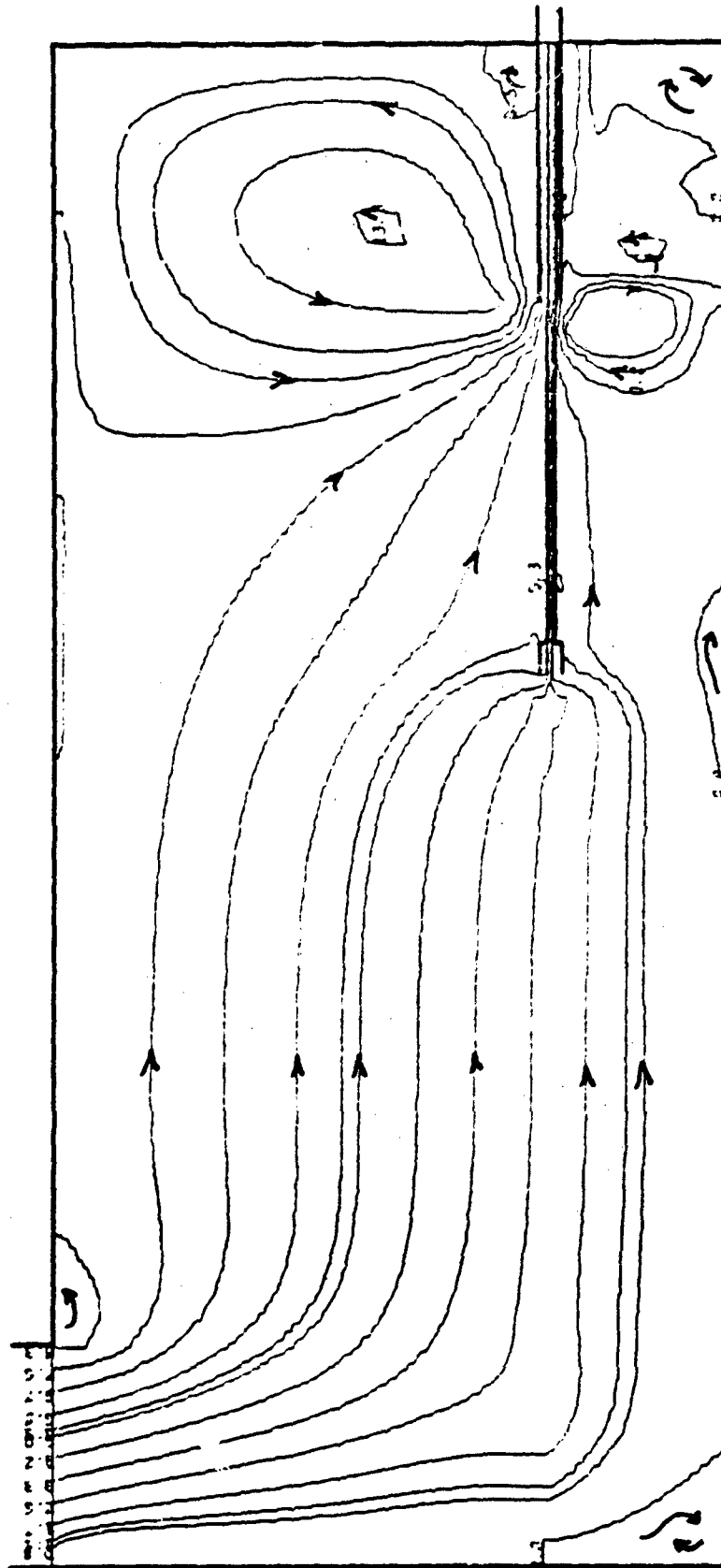
FIGURE 8.   DISTRIBUTION OF STREAMLINES   RUN G4:   Idle RPM,
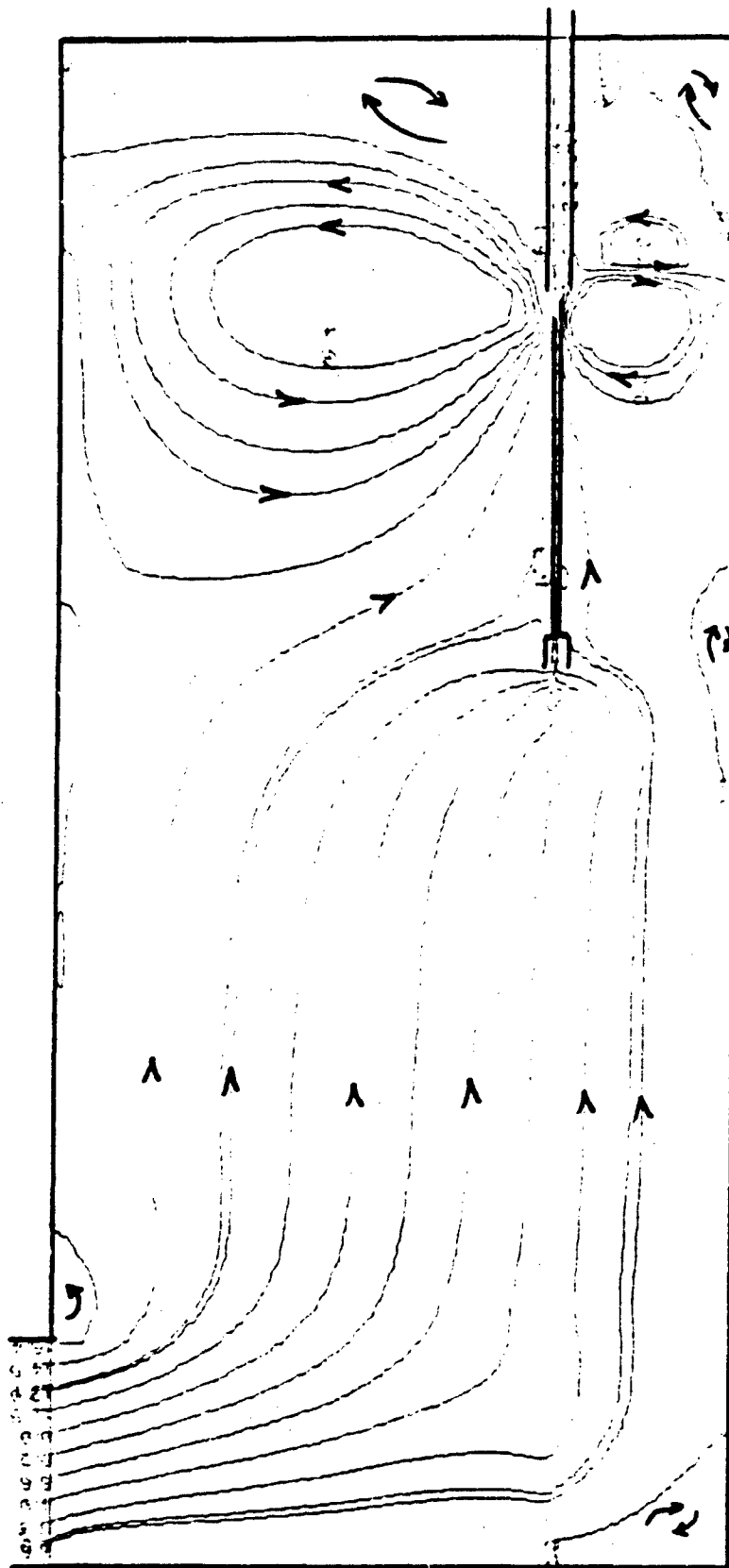
AUGMENTATION RATIO = 1.0:1.
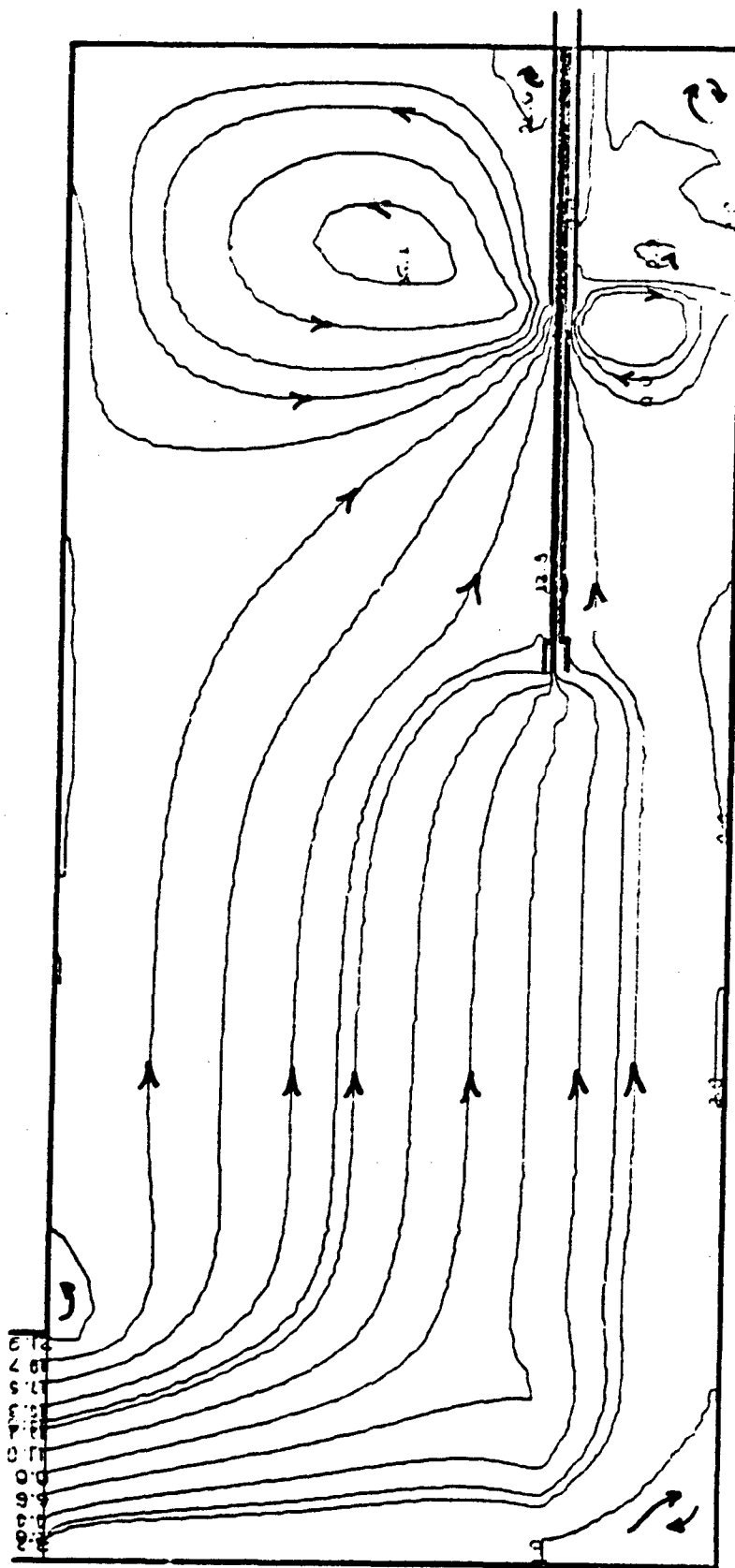
FIGURE 9.   DISTRIBUTION OF STREAMLINES   RUN G1:   100% RPM,
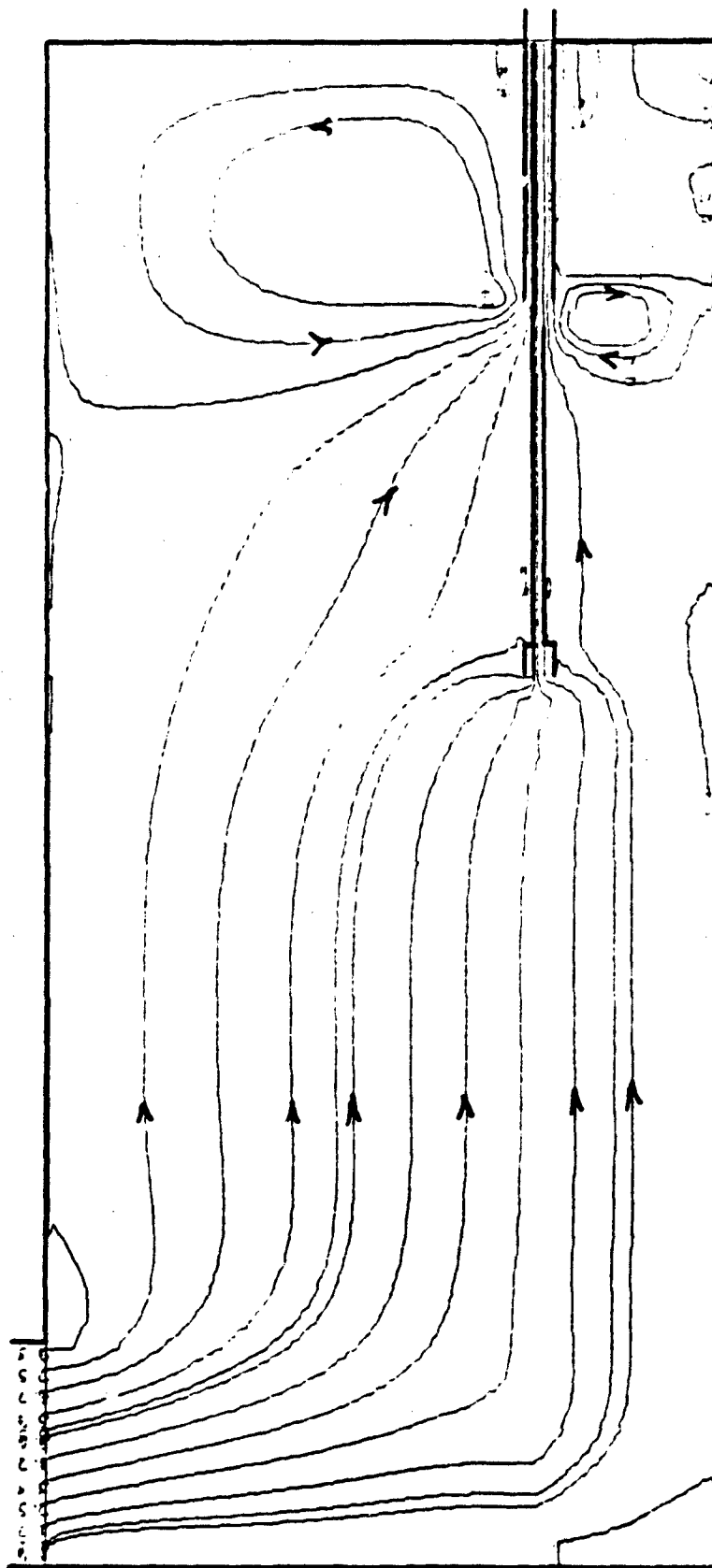
AUGMENTATION RATIO = 1.0:1.

42
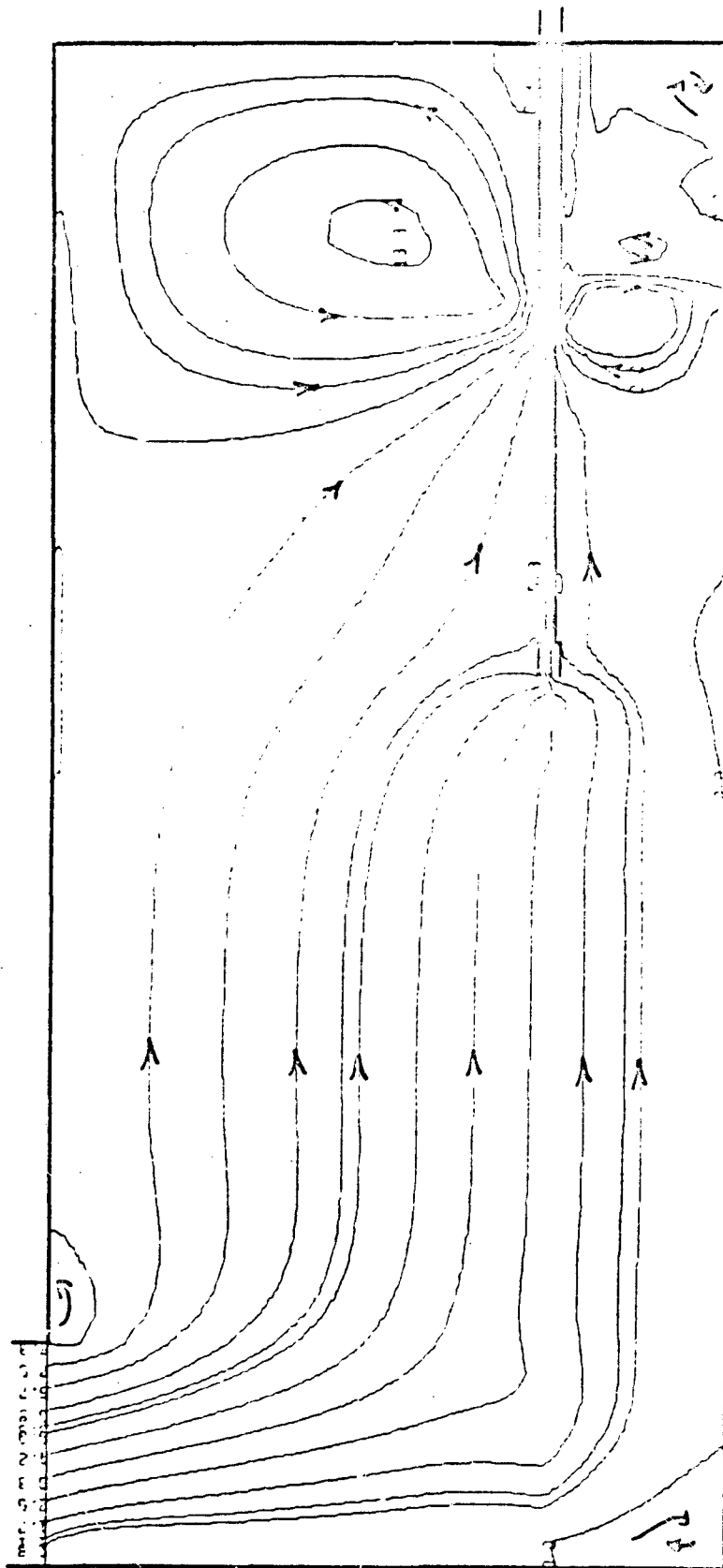
FIGURE 10.   DISTRIBUTION OF STREAMLINES   RUN H8:   Idle RPM,
AUGMENTATION RATIO = 1.0:1.
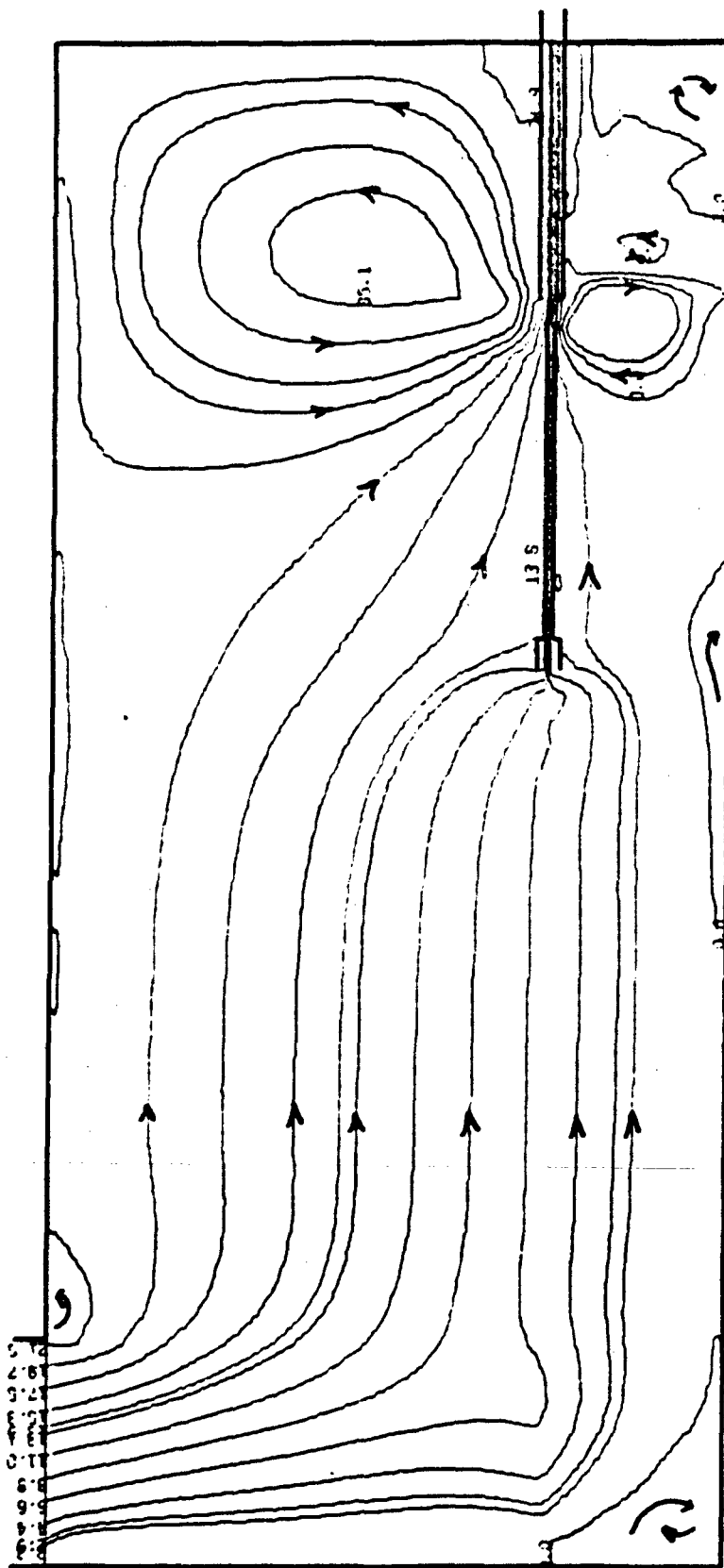
FIGURE 11. DISTRIBUTION OF STREAMLINES RUN !!9: 100% RPM
AUGMENTATION RATIO = 1.0:1.
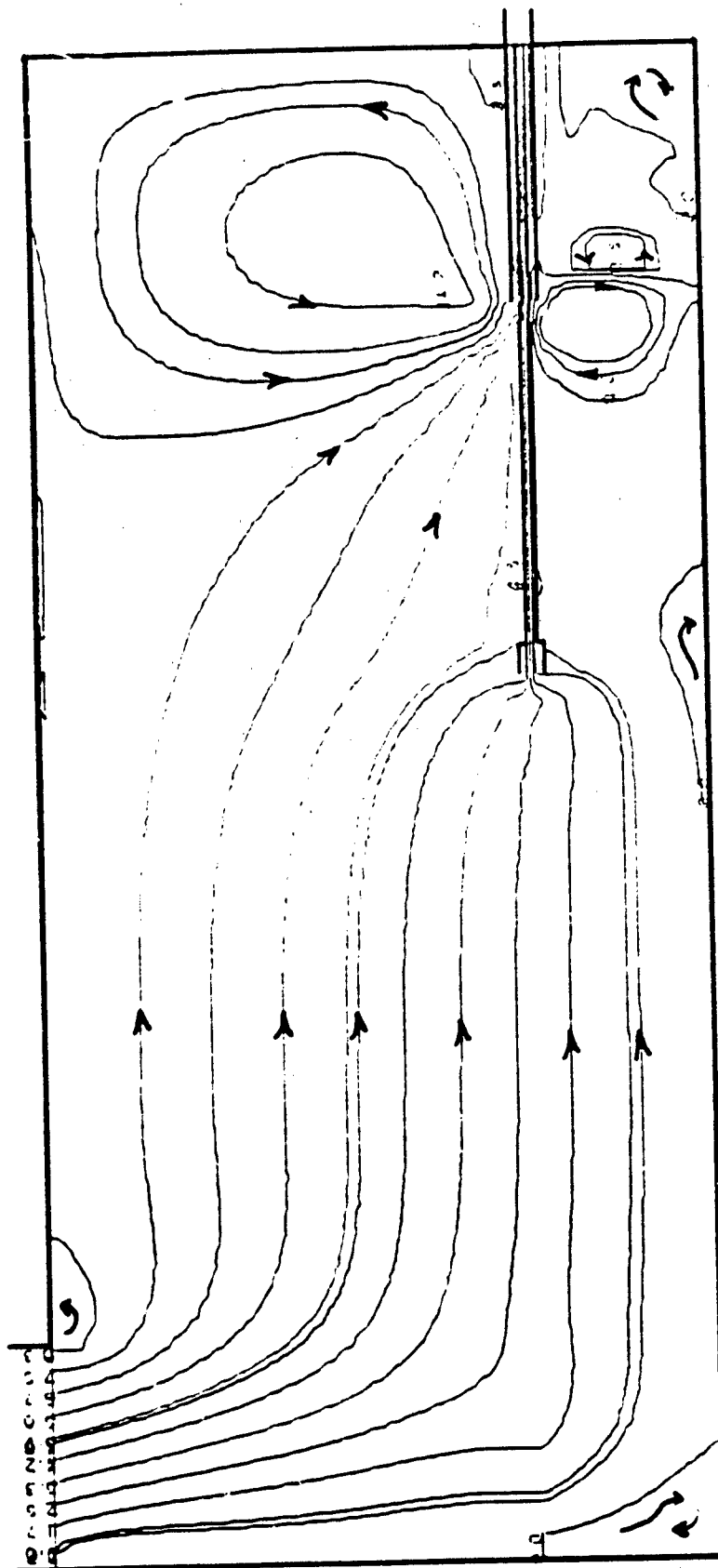
FIGURE 12.   DISTRIBUTION OF STREAMLINES   RUN I1:   Idle RPM,
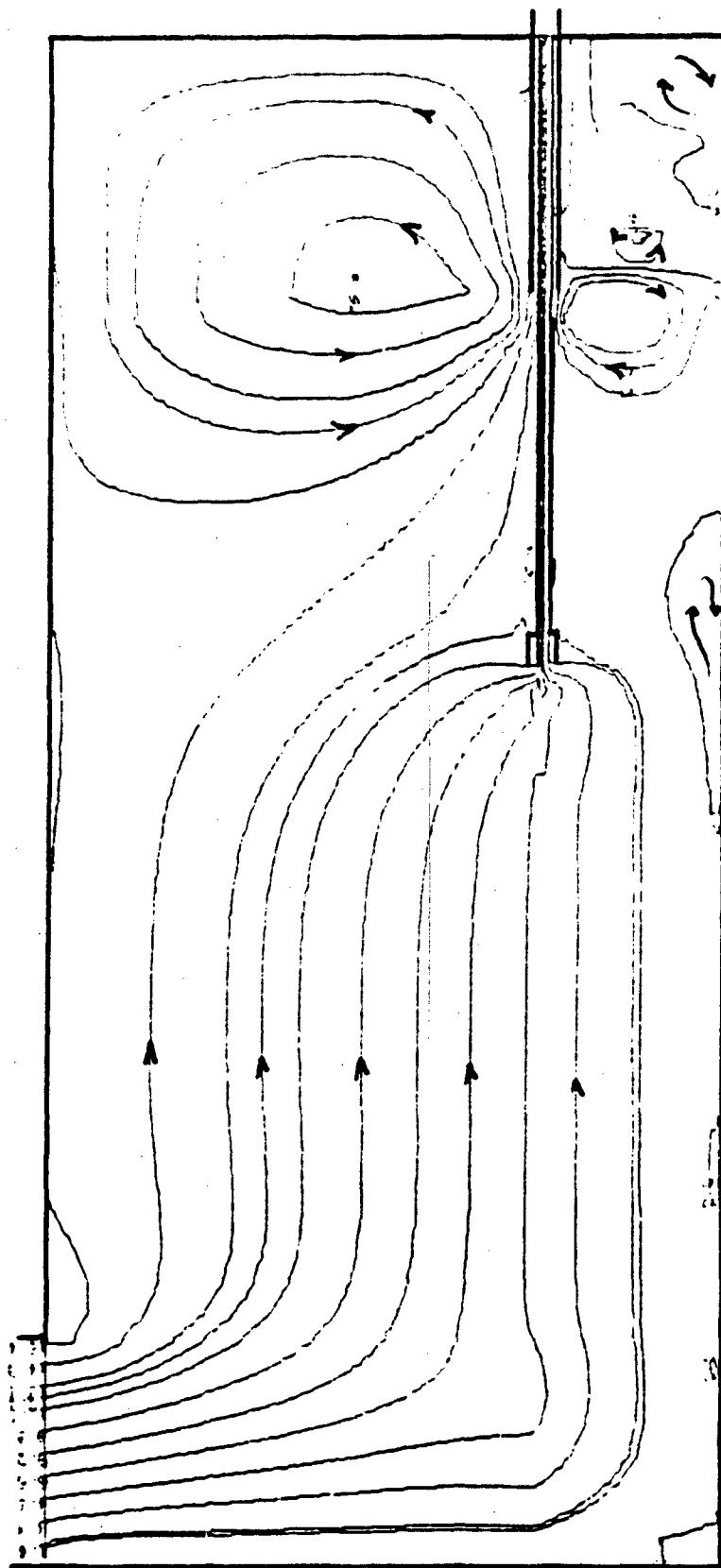
AUGMENTATION RATIO = 1.0:1.
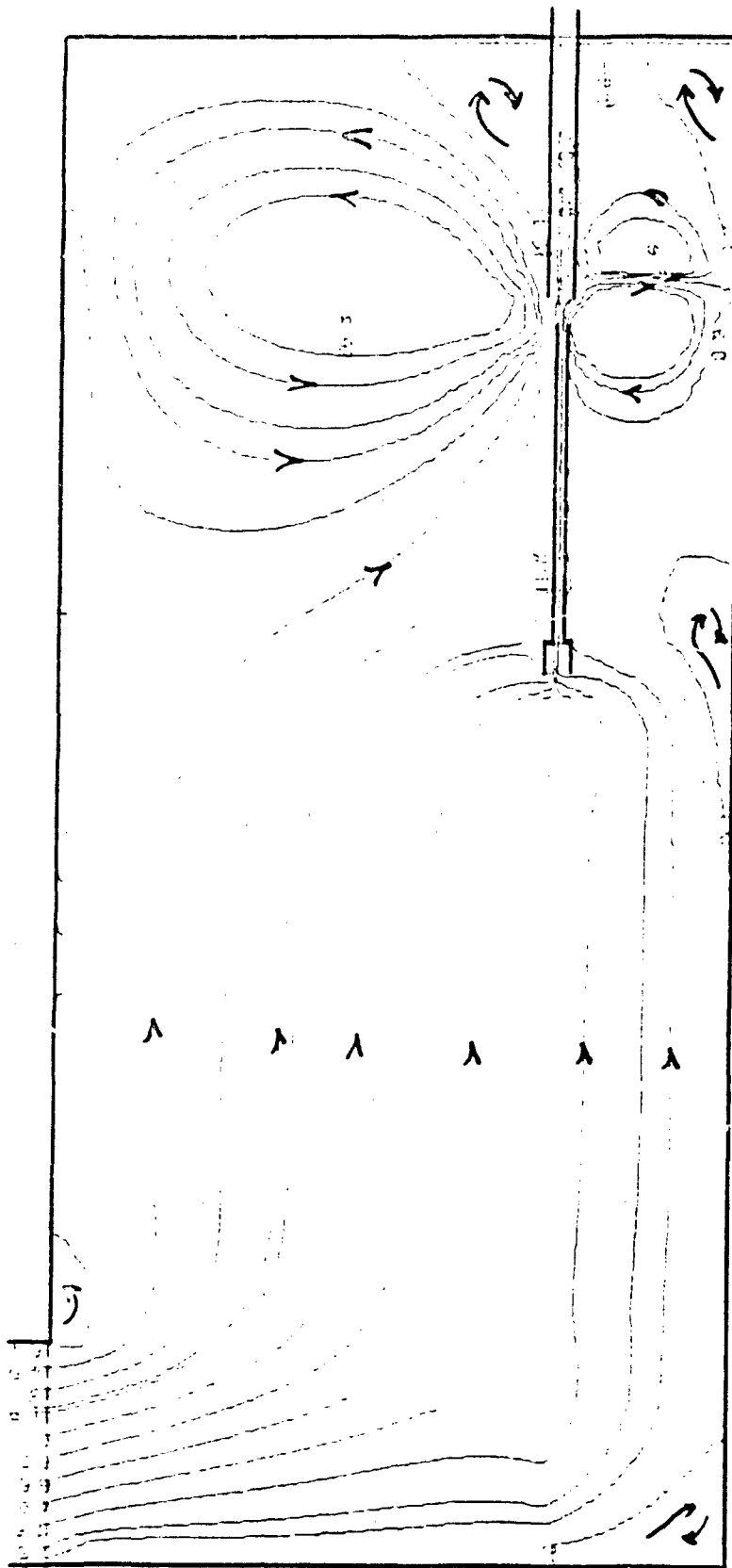
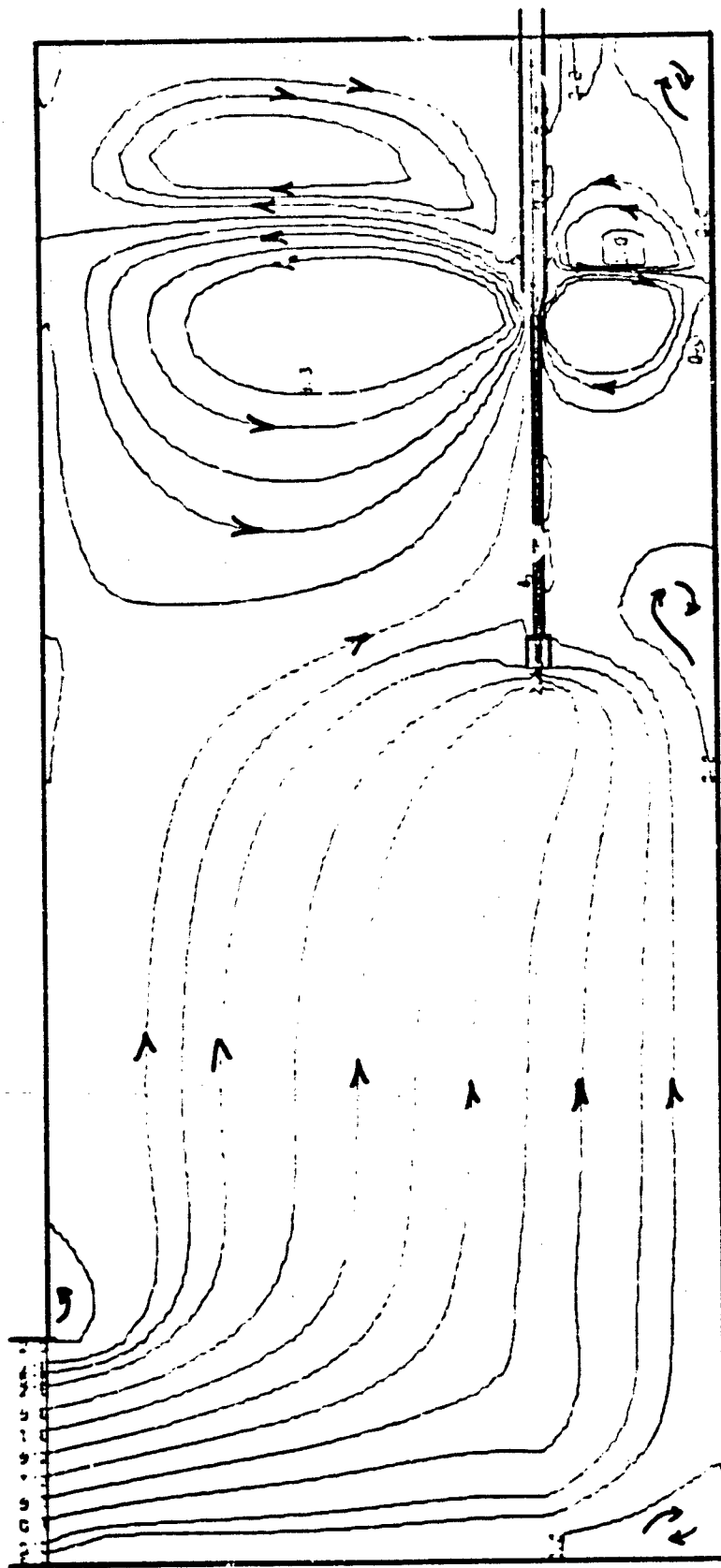FIGURE 13. DISTRIBUTION OF STREAMLINES RUN I2: 1008 RPM, AUGMENTATION RATIO = 1.01.

FIGURE 14. DISTRIBUTION OF STREAMLINES RUN I3: Idle RPM, AUGMENTATION RATIO = 1.0:1.

FIGURE 15. DISTRIBUTION OF STREAMLINES RUN I4: 100% RPM, AUGMENTATION RATIO = 1.0:1.

FIGURE 16.   DISTRIBUTION OF STREAMLINES   RUN L1:   Idle RPM,

AUGMENTATION RATIO = 1.0:1.

FIGURE 17. DISTRIBUTION OF STREAMLINES   RUN L2:   100% RPM,

AUGMENTATION RATIO = .5:1.

FIGURE 18.   DISTRIBUTION OF STREAMLINES   RUN K1:   Idle RPM,
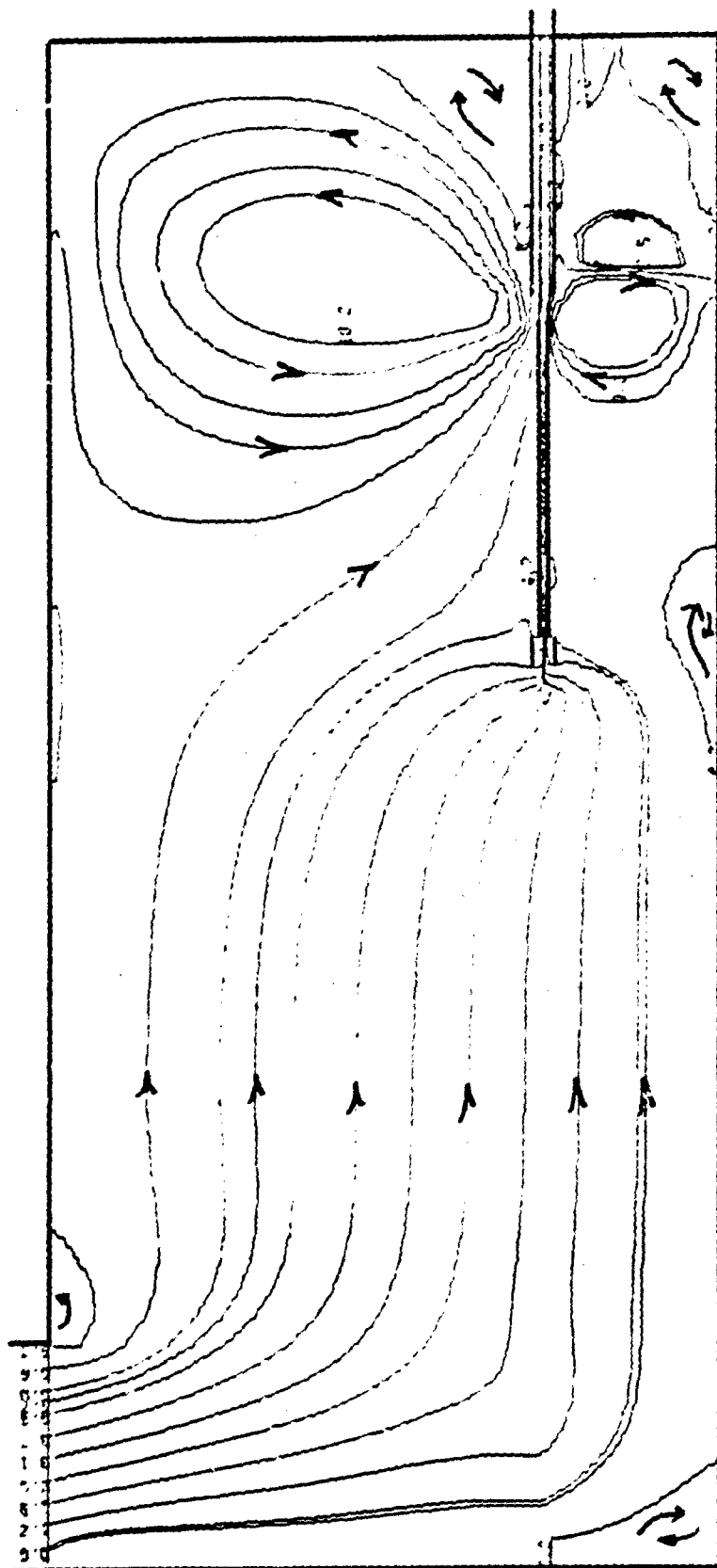
AUGMENTATION RATIO = .25:1.

51

FIGURE 19. DISTRIBUTION OF STREAMLINES   RUN K2:   Idle RPM,
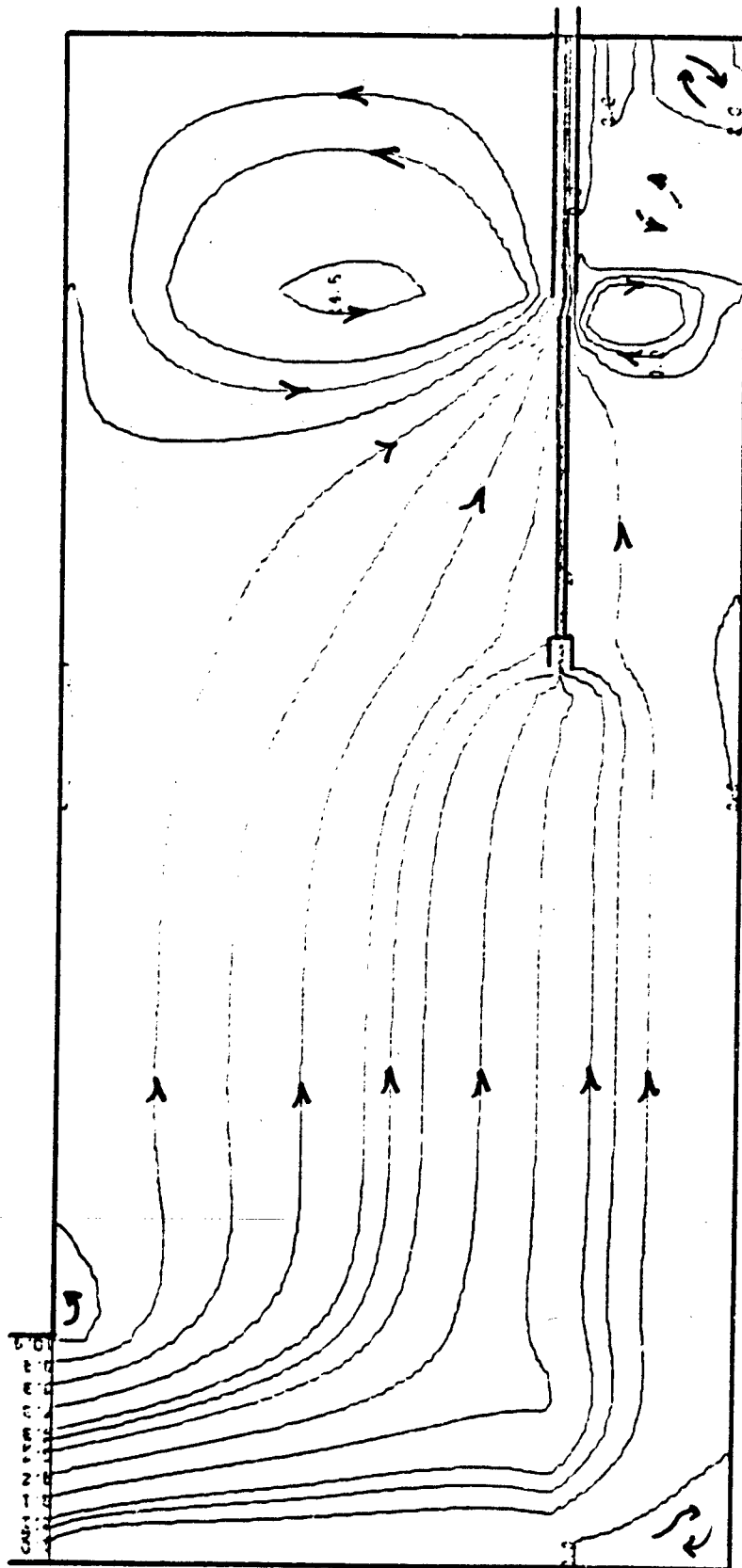
AUGMENTATION RATIO = .5:1.

FIGURE 20. DISTRIBUTION OF STREAMLINES RUN K3: Idle RPM, AUGMENTATION RATIO = 1.5:1.
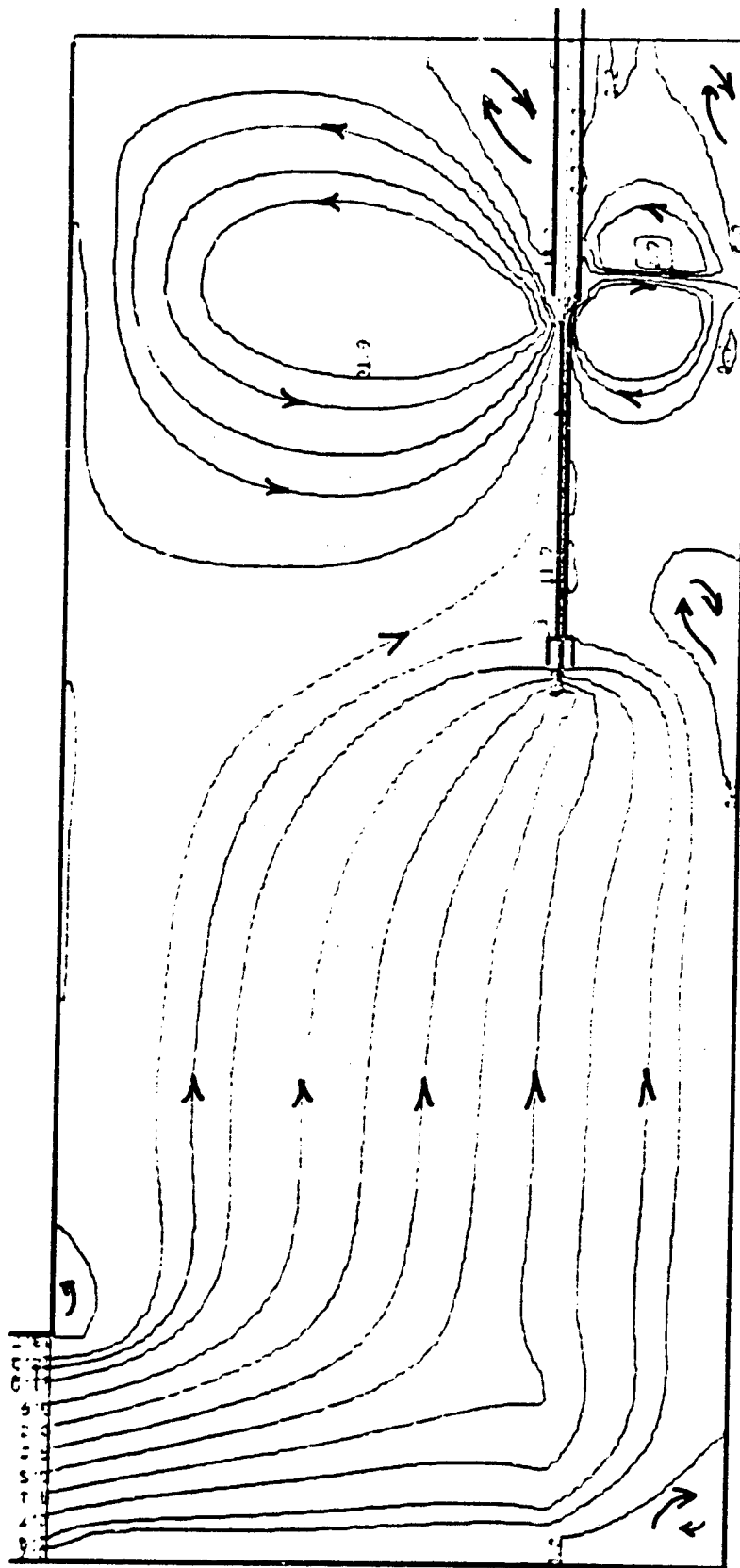
53

FIGURE 21. DISTRIBUTION OF STREAMLINES   RUN K4:   100% RPM
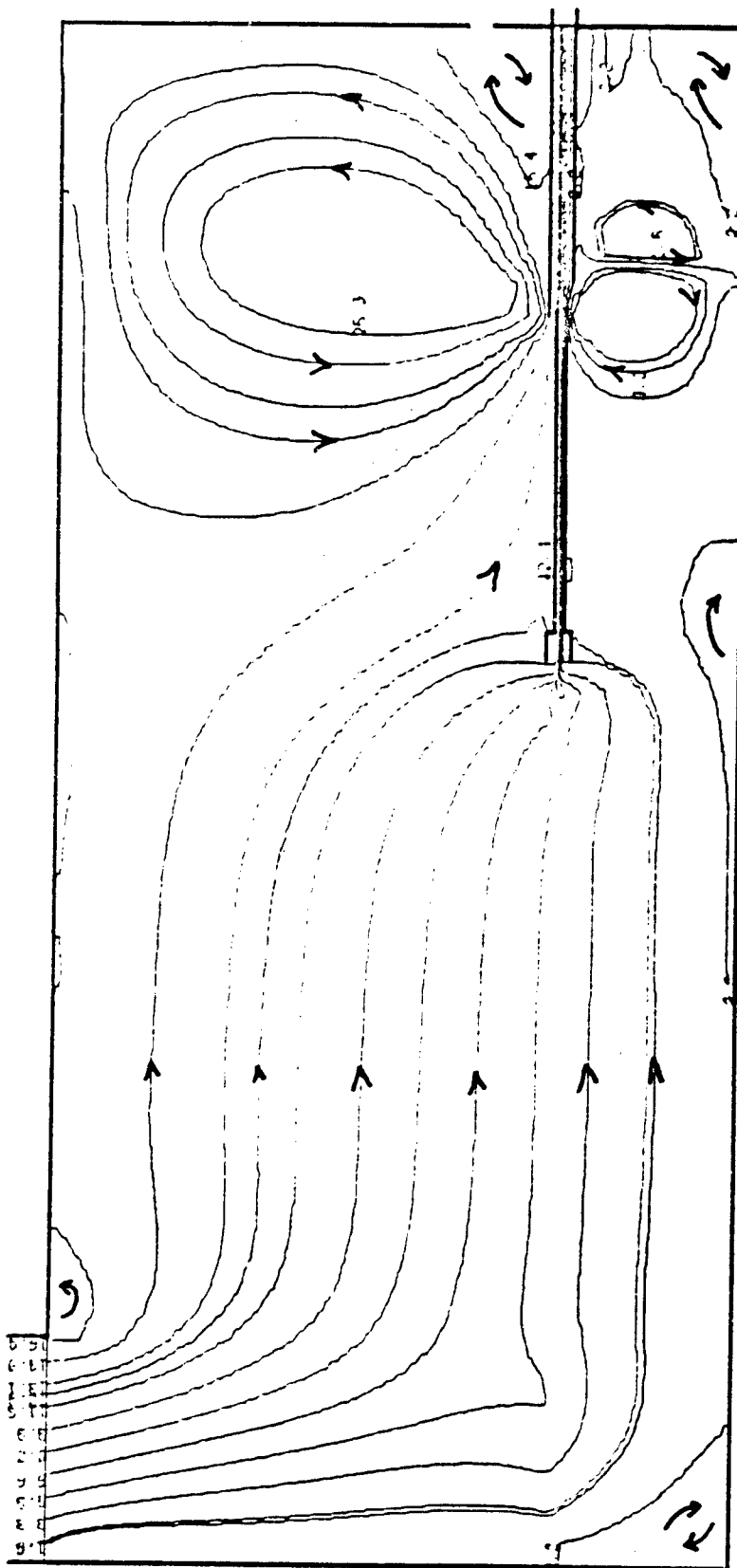
AUGMENTATION RATIO = .25:1.

FIGURE 22.   DISTRIBUTION OF STREAMLINES   RUN K5:   100% RPM,
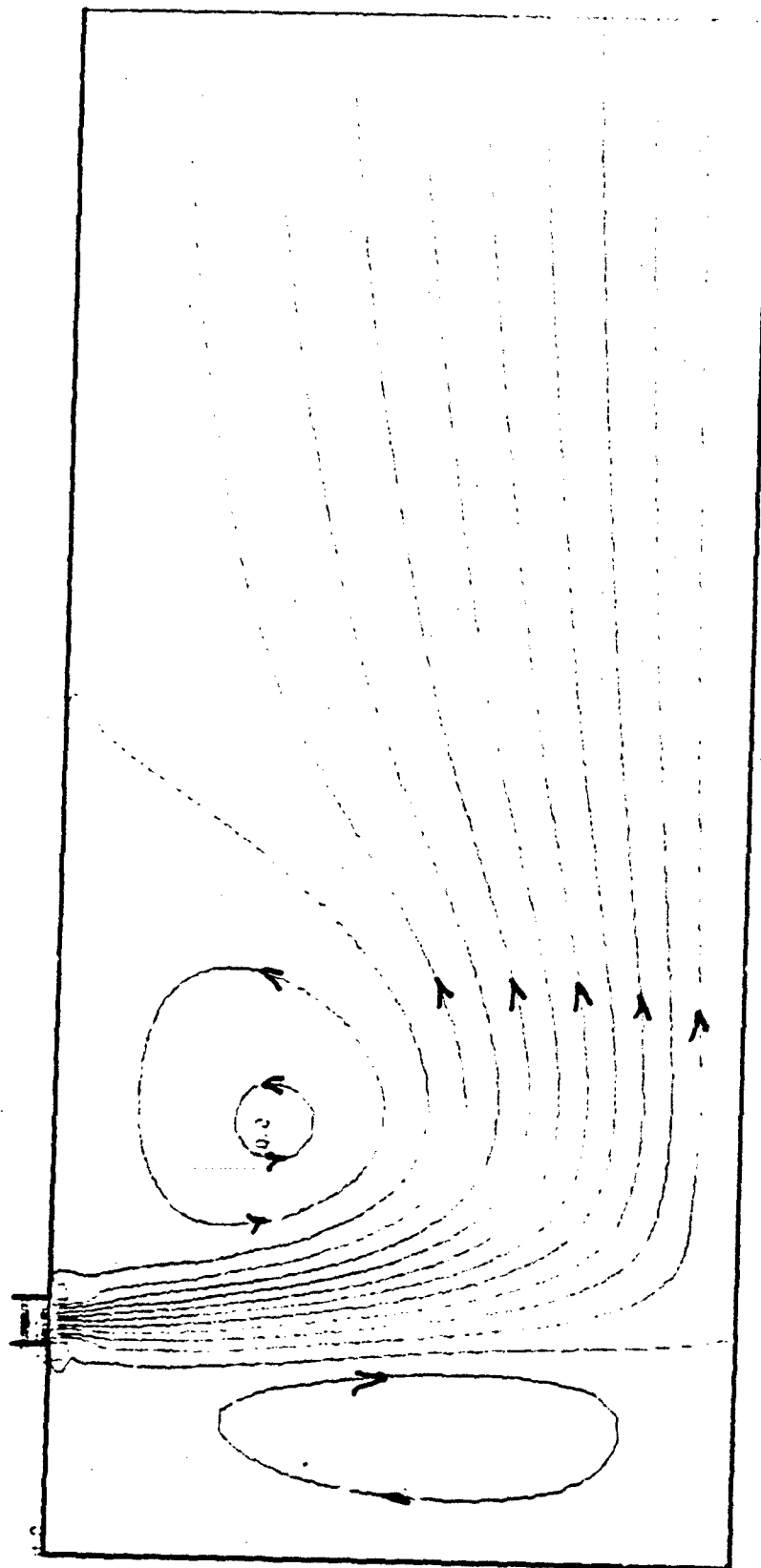
AUGMENTATION RATIO = .5:1.

55

FIGURE 23. DISTRIBUTION OF STREAMLINES IN EXHAUST STACK RUN A2:
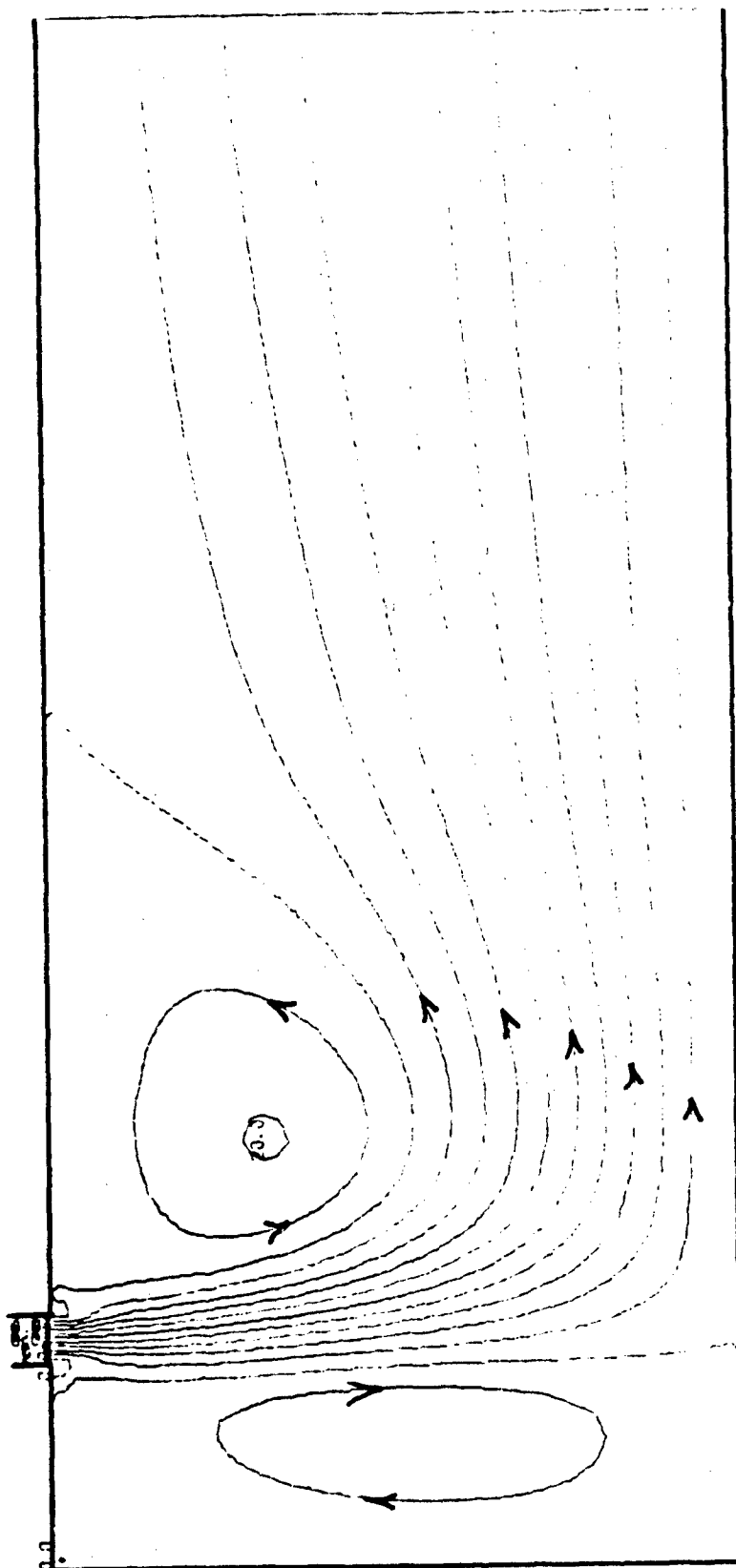AUGMENTER FLUSH, Idle RPM.

FIGURE 24. DISTRIBUTION OF STREAMLINES IN EXHAUST STACK RUN A3:
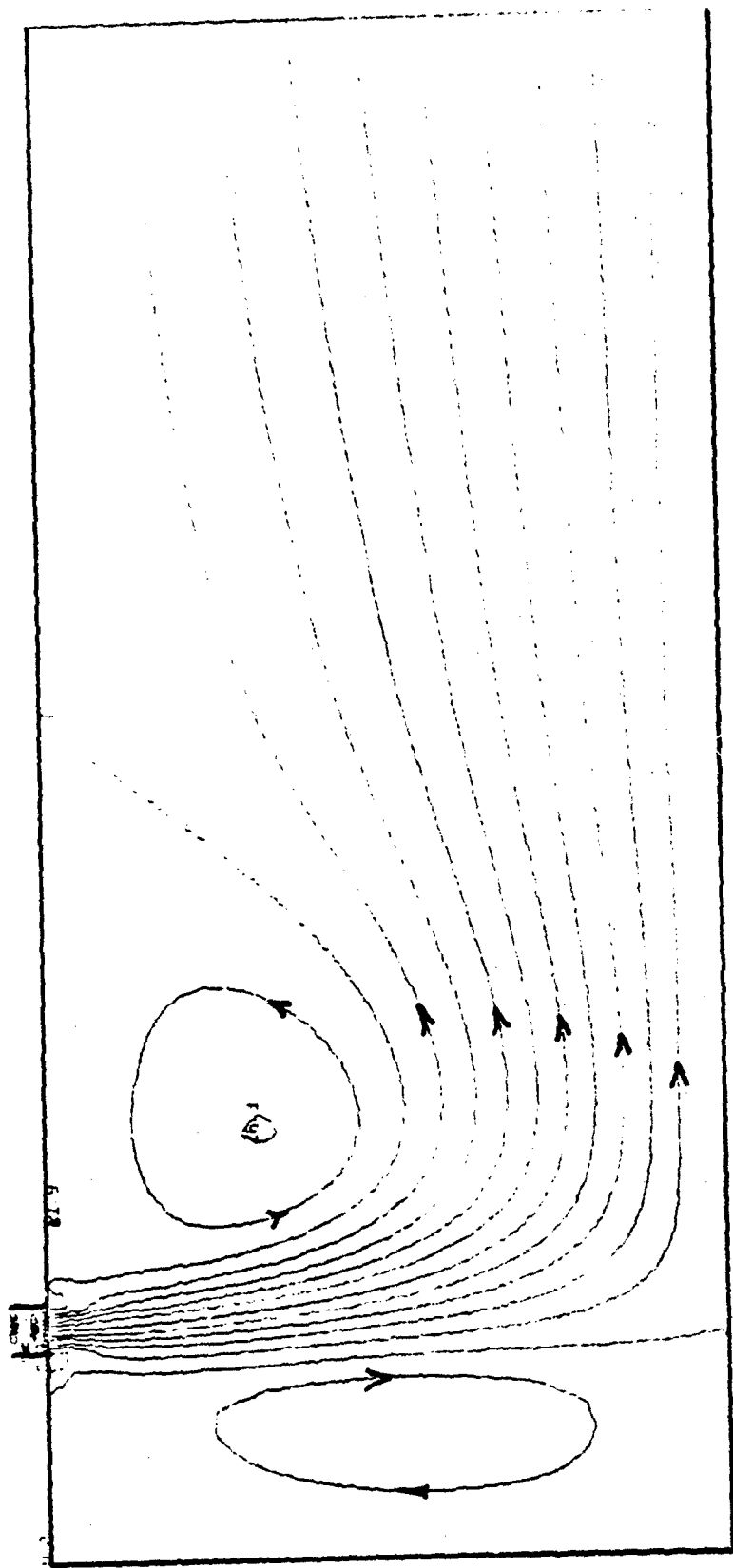AUGMENTER FLUSH, 90% RPM.

FIGURE 25.. DISTRIBUTION OF STREAMLINES IN EXHAUST STACK RUN A4:
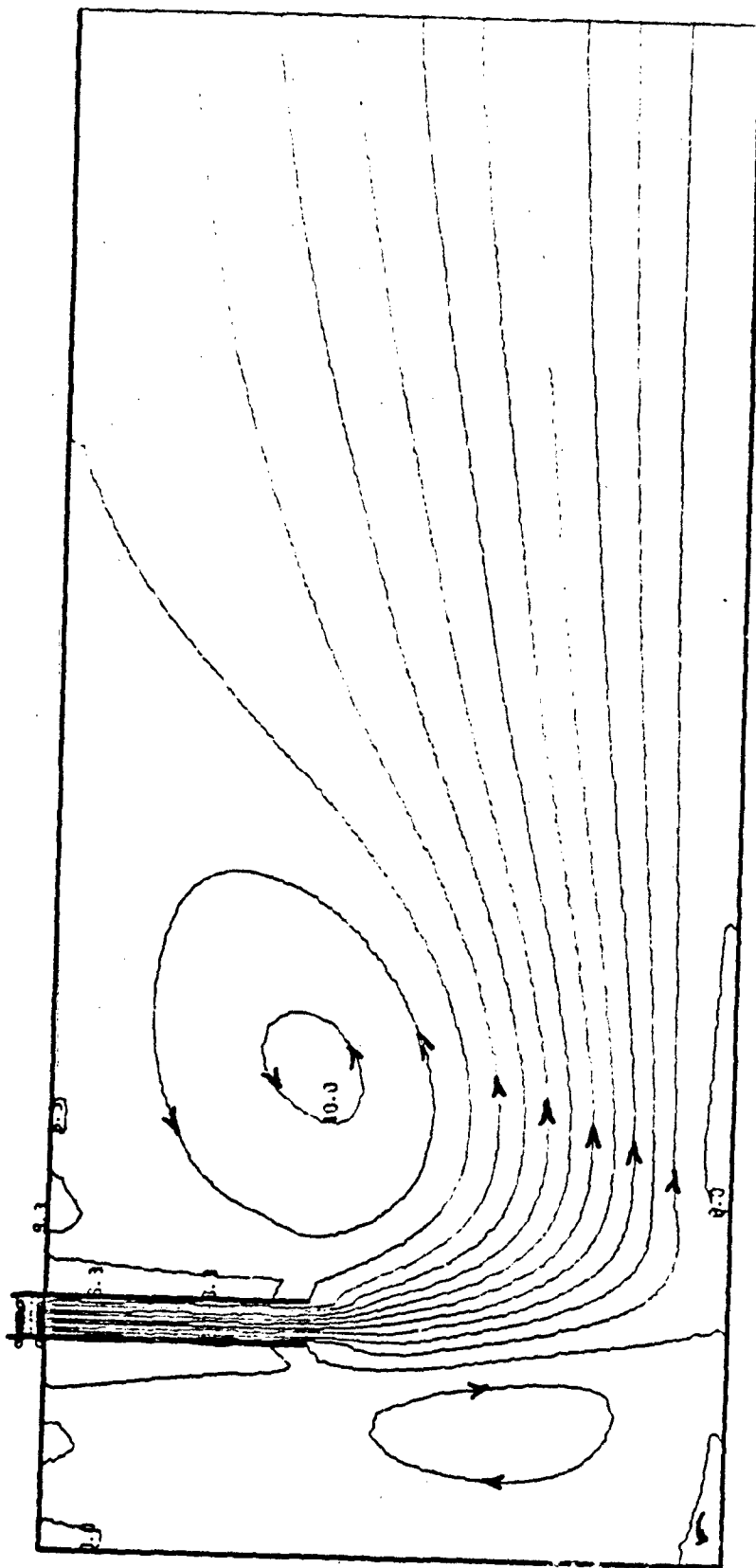
AUGMENTER FLUSH, 100% RPM.

FIGURE 26. DISTRIBUTION OF STREAMLINES IN EXHAUST STACK RUN C2: AUGMENTER EXTENDS FOUR FEET, Idle RPM.
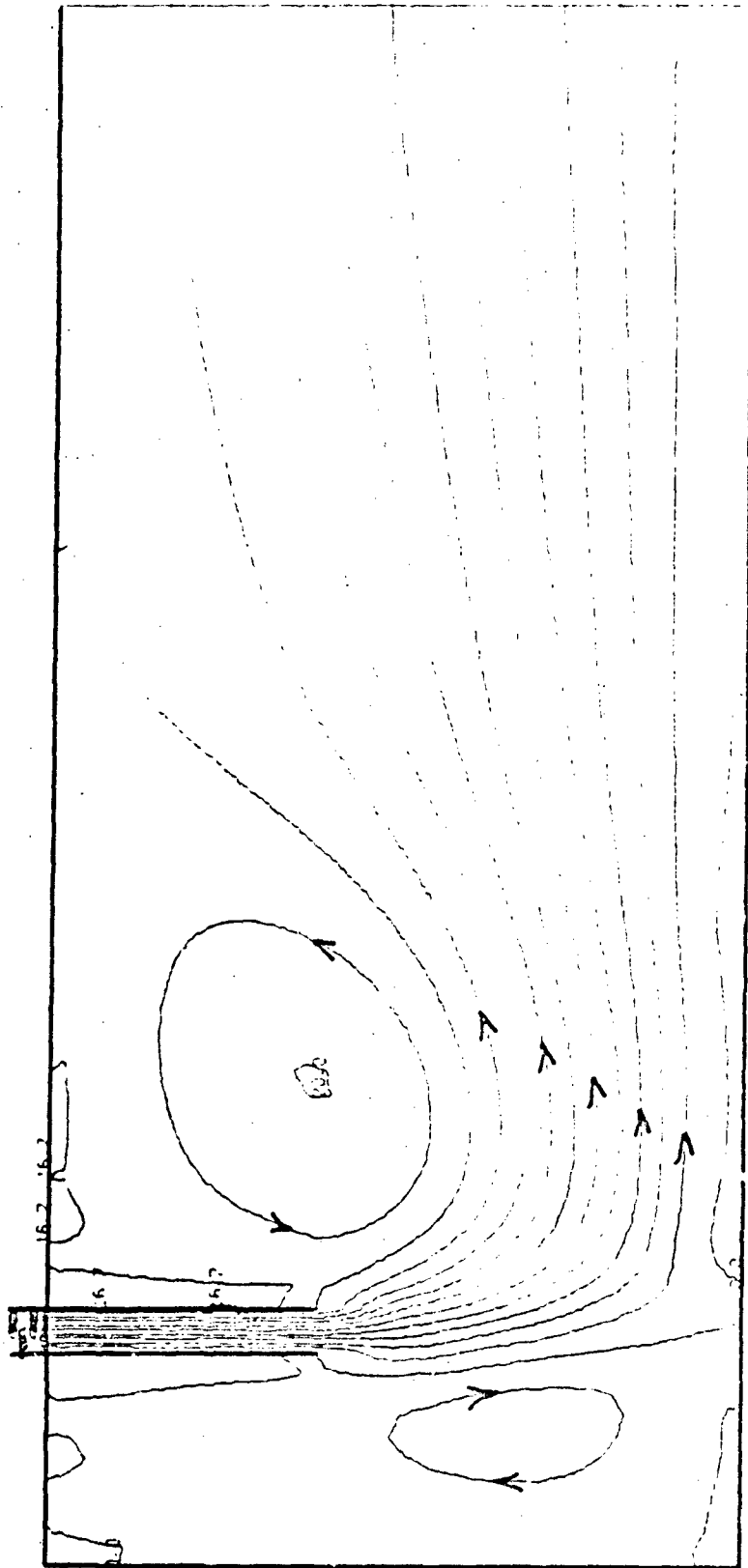
FIGURE 27. DISTRIBUTION OF STREAMLINES IN EXHAUST STACK RUN C3:
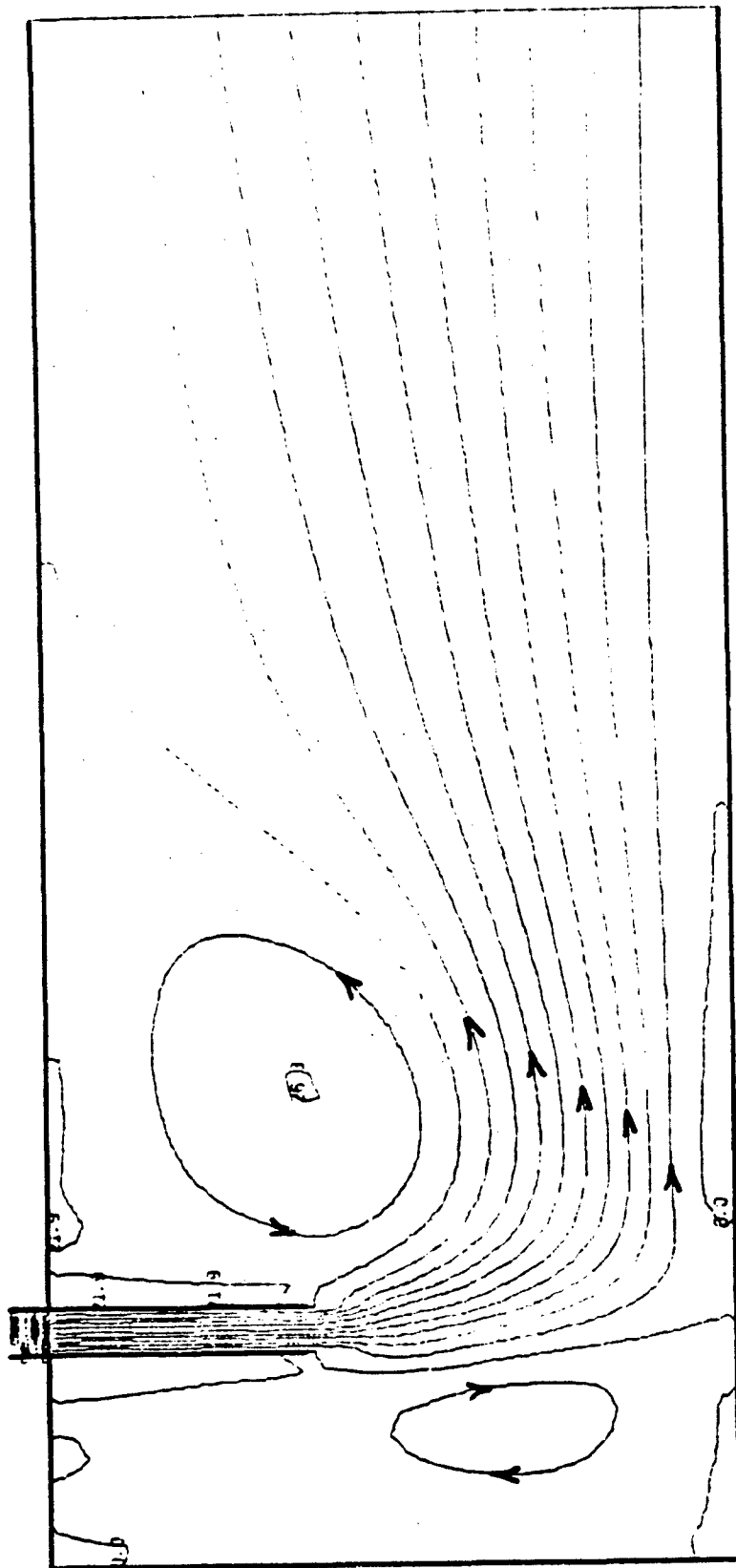AUGMENTER EXTENDS FOUR FEET, 90% RPM.

FIGURE 28. DISTRIBUTION OF STREAMLINES IN EXHAUST STACK RUN C4:
AUGMENTER EXTENDS FOUR FEET, 100% RPM.

61

DISTRIBUTION LIST

No. of Copies

1. Library   2
   Code 0142
   Naval Postgraduate School
   Monterey, CA 93940

2. Department of Aeronautics
   Code 67
   Naval Postgraduate School
   Monterey, CA 93940
        R. W. Bell, Chairman   1
        D. W. Netzer   10

3. Dean of Research   1
   Code 012
   Naval Postgraduate School
   Monterey, CA 93940

4. Defense Documentation Center   2
   Cameron Station
   Alexandria, VA 22314

5. Chief of Naval Operations   2
   Navy Department
   Washington, DC 20360
   (Attn: Codes: OP451, OP453)

6. Chief of Naval Material   2
   Navy Department
   Washington, DC 20360
   (Attn: Codes: 03421, 044P1)

7. Commander   8
   Naval Air Systems Command
   Washington, DC 20361
   (Codes: AIR-01B, 330D, 340E, 4147A,
   50184, 5341B, 53645, 536B1)

8. Commanding Officer   1
   Naval Air Rework Facility
   Naval Air Station North Island
   San Diego, CA 92135
   (Code: 64270)

9. Commander   2
   Naval Facilities Engineering Command
   200 Stovall Street
   Alexandria, VA 22332
   (Codes: 104, 032B)

10. Naval Construction Battalion Center   3
    Port Hueneme, CA 93043)
    (Codes: 25, 251, 252)

11. US Naval Academy   1
    Annapolis, MD 21402
    (Attn: Prof. J. Williams)

12. Arnold Engineering Development Ctr.   1
    Arnold AFS, TN 37342
    (Code: DYR)

13. Air Force Aero Propulsion Laboratory   1
    Wright-Patterson AFB, OH 45433
    (Code: SFF)

14. Air Force Civil Engineering Center   2
    Tyndall AFB, FL 32401
    (Code: EV, EVA)

15. Army Aviation Systems Command   1
    P. O. Box 209
    St. Louis, MO 63166
    (Code: EQP)

16. Eustis Directorate   1
    USA AMR & DL
    Ft. Eustis, VA 23604
    (Code: SAVDL-EU-TAP)

17. National Aeronautics and Space Admin.   1
    Lewis Research Center
    2100 Brookpark Road
    Cleveland, OH 44135
    (Attn: Mail Stop 60-6 (R. Rudley))

18. Federal Aviation Administration   1
    National Aviation Facility Experimental Ctr.
    Atlantic City, NJ 08405

19. Naval Air Propulsion Test Center   1
    Trenton, NJ 08628
    (Code PE71:AFK)